NUMERICAL APPROXIMATION METHODS

1. Numerical approximation

The velocity v is such that

$$v(0) = v_{max}, \quad v(\rho_{max}) = 0.$$

As the velocity is a linear function, the maximum $\sigma \in (0, \rho_{max})$ is unique for the flux:

$$f(\sigma) = \max_{[0,\rho_{max}]} f(\rho) = f_M.$$

The flux is:

$$f(\rho) = v_{max}\rho\left(1 - \frac{\rho}{\rho_{max}}\right)$$

where we set for simplicity $\rho_{max} = 1 = v_{max}$, thus it reads:

$$f(\rho) = \rho(1 - \rho).$$

The graph in Fig. 1 represents the flux function $f(\rho)$. In order

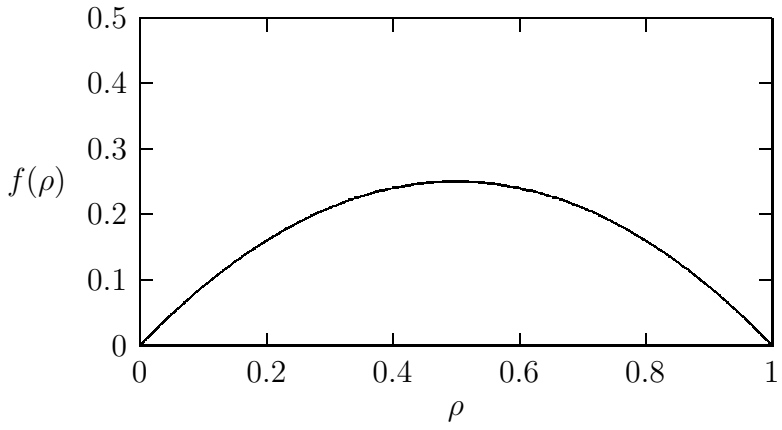

Figure 1. The flux function.

to produce approximated solutions to these problems, we use some numerical methods, such as Godunov and relaxation type schemes, which are analyzed in the context of the traffic model we deal with. In particular, the new contribute is represented by the study and elaboration of suitable boundary conditions for all of these schemes.

1.1. **Godunov's method.**
We define a numerical grid in $\mathbb{R}^N \times (0,T)$ using the following notations:

- Δx is the space grid size;
- Δt is the time grid size;
- $(x_m, t_n) = (m\Delta x, n\Delta t)$ for $n \in \mathbb{N}$ and $m \in \mathbb{Z}$ are the grid points.

For a function v defined on the grid we write $v_m^n = v(x_m, t_n)$. We also use the notation u_m^n for $u(x_m, t_n)$ when u is a continuous function on the (x,t) plane and $\tilde{v}$ for the vector of v values, $(v_m^n)_{m,n}$ for m and n varying on a subset of $\mathbb{Z}$ and $\mathbb{N}$ respectively.
The method obtained by the procedure described below is known as Godunov's method and was introduced in 1959 as an approach to solving the Euler equations of gas dynamics in the presence of shock waves. For the detailed description of this scheme see [6]. This method is based on the solution of local Riemann's problems. Recall that the (unique) solution of the Riemann's problem

$$u_t + F(u)_x = 0 \qquad x \in \mathbb{R}, \quad t \in [0,T], \tag{1.1}$$

with initial data

$$u(x,0) = u_0(x) = \begin{cases} u_l \text{ if } x < 0, \\ u_r \text{ if } x > 0, \end{cases} \tag{1.2}$$

is self-similar, that is to say

$$u(x,t) = W_R(x/t; u_l, u_r),$$

where W_R depends only on the flux function F and consists of the two constant states u_l and u_r, separated by various waves starting from the origin whose speeds are bounded by

$$\max\{|F'(\xi)|, \xi \text{ between } u_l \text{ and } u_r\}.$$

We search for an approximated solution of the given problem.
Assign an initial data $u_0(x)$ and approximate it by v^Δ, that represents a piecewise constant function defined a. e. in $\mathbb{R} \times (0, +\infty)$.
1 step. The initial data is approximated by the sequence $v^0 = (v_m^0)$ in the following way

$$v_m^0 = \frac{1}{\Delta x} \int_{x_{m-1/2}}^{x_{m+1/2}} u_0(x)dx. \tag{1.3}$$

Then the function v_Δ is

$$v_0^\Delta(x) = v_m^0, \quad x \in (x_{m-1/2}, x_{m+1/2}), \ m \in \mathbf{Z}.$$

Analogously, given an approximation v_m^n of u at time $t = t_n$, we set

$$v^\Delta(x, t_n) = v_m^n, \quad x \in (x_m - 1/2, x_{m+1/2}), \ m \in \mathbf{Z}.$$

The scheme defines v_m^n recursively starting from v_m^0.
Let $v^\Delta(x,t)$ be the solution of the problem:

$$\begin{cases} \partial_t v + \partial_x F(v) = 0 & x \in \mathbb{R}, t \in (t_n, t_{n+1}), \\ v(x,t_n) = v^\Delta(x,t_n). \end{cases} \tag{1.4}$$

As v_Δ belongs to $L^\infty(\mathbb{R})$, the problem admits a unique entropy solution that can be determined explicitely at least for Δt small enough.

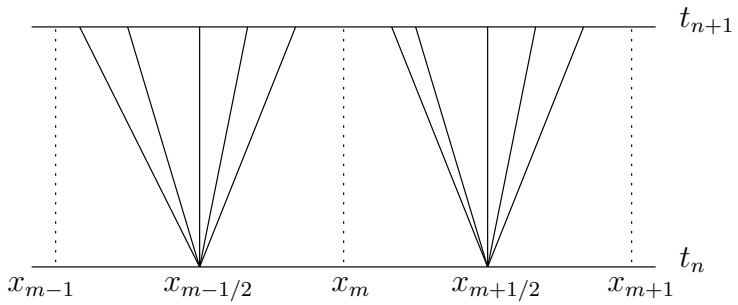

Remark 1.1 If

$$\Delta t \sup_{m,n} \left\{ \sup_{u \in I(u^n_{m-1/2}, u^n_{m+1/2})} |F'(u)| \right\} \leq \frac{1}{2}\Delta x \tag{1.5}$$

a wave starting from $x_{m-1/2}$ will not reach the lines $x = x_{m-1}$ and $x = x_m$ before time t_{n+1}.

■

2 step. Now we define, as natural

$$v_m^{n+1} = \frac{1}{\Delta x} \int_{x_{m-1/2}}^{x_{m+1/2}} v^\Delta(x, t_{n+1}) dx, \tag{1.6}$$

which represents the projection of the exact solution on a piecewise constant function. To get a simple expression for v_m^{n+1}, we use the Gauss-Green formula to integrate (1.1) on the cell $(x_{m-1/2}, x_{m+1/2}) \times (0, \Delta t)$. This is possible since u is piecewise smooth and satisfies the Rankine-Hugoniot condition at the discontinuities. One has

$$\begin{aligned} 0 \;=\; & \int_{t_n}^{t_{n+1}} \int_{x_{m-1/2}}^{x_{m+1/2}} (\partial_t v + \partial_x F(v)) dx dt \\ & \int_{x_{m-1/2}}^{x_{m+1/2}} [v(x, t^{n+1}) - v(x, t^n)] dx + \int_{t_n}^{t_{n+1}} [F(v(x_{m-1/2}, t)) - F(v(x_{m+1/2}, t))] dt. \end{aligned} \tag{1.7}$$

Under the CFL condition

$$\Delta t \sup_{m,n} \left\{ \sup_{u \in I(u^n_{m-1/2}, u^n_{m+1/2})} |F'(u)| \right\} \leq \Delta x, \tag{1.8}$$

the waves do not influence the solutions in $x = x_{m+1/2}$, for $t \in (t_n, t_{n+1})$. Hence the solutions are locally given by the Riemann's problems and in particular the flux in $x = x_{m+1/2}$ for $t \in (t_n, t_{n+1})$ is given by

$$F(u(x_m, t)) = F(W_R(0; v^n_{m-1}, v^n_m)).$$

Since the flux is time invariant and continuous, we can put it out of the integral and obtain:

$$v^{n+1}_m = v^n_m - \frac{\Delta t}{\Delta x}\left(F(W_R(0; v^n_m, v^n_{m+1}) - F(W_R(0; v^n_{m-1}, v^n_m))\right). \tag{1.9}$$

We have

$$g^G(u, v) = F(W_R(0; u, v)),$$

so the numerical flux g^G has the expression

$$g^G(u,v) = \begin{cases} \min_{w\in[u,v]} F(w) & \text{if } \ u \le v, \\ \\ \max_{w\in[v,u]} F(w) & \text{if } \ v \le u. \end{cases}$$

In particular, for the flux we are considering:

$$g^G(u,v) = \begin{cases} \min(F(u), F(v)) & \text{if } u \le v, \\ \\ F(u) & \text{if } v < u < \sigma, \\ \\ F(\sigma) & \text{if } v < \sigma < u, \\ \\ F(v) & \text{if } \sigma < v < u. \end{cases}$$

The scheme, under the condition (1.8), can be written in the form

$$v^{n+1}_m = v^n_m - \frac{\Delta t}{\Delta x}\big(g^G(v^n_m, v^n_{m+1}) - g^G(v^n_{m-1}, v^n_m)\big). \tag{1.10}$$

1.1.1. *Boundary conditions.* Suppose to assign a condition at the incoming boundary $x = 0$:

$$u(0, t) = \rho_b(t) \quad t > 0$$

and study equation only for $x > 0$. Now we are considering the initial-boundary value problem

$$\begin{cases} u_t + F(u)_x = 0 & x \in I \quad t \in [0, T], \\ u(x, 0) = u_0(x) & x \in I, \\ u_x(0, t) = u_b(t) & t \in [0, T], \end{cases}$$

with I an open interval strictly contained in $\mathbb{R}$, $u_0 \in C^1(I)$, $u_1(t) \in C^1((0, T))$, $F \in C^1(\mathbb{R})$. It is not easy to find a function u that satisfies (1.1.1) in a classical sense, because, in general, the boundary data cannot be assumed. Consider, for instance, the scalar problem

$$\begin{cases} u_t - u_x = 0 & \mathbb{R}^+ \times (0, T), \\ u(x, 0) = u_0(x) & \mathbb{R}^+ \times \{0\}. \end{cases} \tag{1.11}$$

This problem admits a unique global solution $u(x,t) = u_0(x+t)$ in $(0,+\infty)\times(0,+\infty)$, thus condition

$$u(0,t) = u_b(t), \quad t \geq 0 \tag{1.12}$$

is not consistent. On the other side, for the problem

$$\begin{cases} u_t + u_x = 0 & \mathbb{R}^+ \times (0,T), \\ u(x,0) = u_0(x) & \mathbb{R}^+ \times \{0\}, \end{cases} \tag{1.13}$$

condition (1.12) is needed to be imposed. From the example above, it is evident that the necessity of prescribing the boundary condition is connected to the flux structure. Generally, one seeks a condition which is to be effective only in the inflow part of the boundary.
The rigorous way of assigning the boundary condition is given in [3]. From this condition, using that $u(0,t) \neq u_b(t)$ we deduce that $F'(u(0,t)) \leq 0$: this means that characteristic line is outgoing. Therefore, the boundary condition applies when $F'(u_b) > 0$. So, we have

$$u(0,t) = u_b(t)$$

only for the values of t such that $F'(u(0,t)) > 0$.
We practically proceed by inserting a ghost cell and defining

$$v_0^{n+1} = v_0^n - \frac{\Delta t}{\Delta x}\big(g^G(v_0^n, v_1^n) - g^G(u_1^n, v_0^n)\big), \tag{1.14}$$

where

$$u_1^n(t) = \frac{1}{\Delta t}\int_{t_n}^{t_{n+1}} \rho_b(t)dt$$

takes the place of v_{-1}^n.
An outgoing boundary can be treated analogously. Let $x < L = x_N$. Then the (formal) condition is:

$$u(L,t) = \rho_2(t)$$

and the discretization reads:

$$v_N^{n+1} = v_N^n - \frac{\Delta t}{\Delta x}\big(g^G(v_N^n, u_2^n) - g^G(v_{N-1}^n, v_N^n)\big), \tag{1.15}$$

where

$$u_2^n(t) = \frac{1}{\Delta t}\int_{t_n}^{t_{n+1}} \rho_2(t)dt$$

takes the place of v_{N+1}^n, that is a ghost cell value.

1.1.2. *Conditions at a junction.* Recall that $\hat{\gamma}_i$ and $\hat{\gamma}_j$ are the maximized fluxes where the subscript i indicates the incoming roads and the subscript j the outgoing roads.
For roads connected to a junction at the right endpoint we set

$$v_N^{n+1} = v_N^n - \frac{\Delta t}{\Delta x}\big(\hat{\gamma}_i - g^G(v_{N-1}^n, v_N^n)\big),$$

while for roads connected to a junction at the right endpoint we have

$$v_0^{n+1} = v_0^n - \frac{\Delta t}{\Delta x}\big(g^G(v_0^n, v_1^n) - \hat{\gamma}_j\big).$$

Remark 1.2 For the Godunov's scheme there is no need to invert the flux f to put it in the scheme, as the Godunov's flux coincides with the Riemann's flux. In this case it suffices to insert the computed maximized fluxes directly in the scheme.

■

2. Discretization of the Relaxation Methods

Consider a BGK approximation. Given the following Cauchy problem for a scalar one-dimensional conservation law

$$u_t + F(u)_x = 0 \quad \text{in } \mathbb{R} \times (0, \infty), \tag{2.1}$$

$$u(x, 0) = u_0(x) \quad \text{on } \mathbb{R} \times \{t = 0\}, \tag{2.2}$$

it is approximated by introducing a uniform grid $[x_{m-1/2}, x_{m+1/2}] \times [t_n, t_{n+1}]$ such that

- Δx is the space grid size;
- Δt is the time grid size;
- $(x_m, t_n) = ((m + 1/2)\Delta x, n\Delta t)$ for $n \in \mathbb{N}$ and $m \in \mathbb{Z}$ are the grid points.

The system to be discretized is

$$\begin{cases} \partial_t f^k + \lambda_k \partial_x f^k = \frac{1}{\varepsilon}(M_k(u) - f_k), & k = 1, \dots, N \\ f_k(x, 0) = M_k(u_0(x)), & t = 0,\ x \in \mathbb{R}^+. \end{cases}$$

In order to avoid the initial layer effect we put the state of equilibrium as the initial data

$$f_{\varepsilon,k}^{m,0} = M_k(u_0^m)$$

and, in general, on the cell we have

$$f_{\Delta,k}^{\varepsilon} = f_{\varepsilon,k}^{m,n},$$

where $f^{m,n}$ is an approximation of

$$\frac{1}{\Delta x}\int_{x_{m-1/2}}^{x_{m+1/2}} F(x, t_n)dx$$

and the initial data of problem is discretized by

$$u_m^0 = \frac{1}{\Delta x}\int_{x_{m-1/2}}^{x_{m+1/2}} u_0(x)dx, \quad m \in \mathbb{N}.$$

To discretize the system above we need to solve a diagonal linear problem

$$\begin{cases} \partial_t f^k + \lambda_k \partial_x f^k = 0, & k = 1, \dots, N \\ F(x, 0) = f_k^n(x). \end{cases}$$

These are N equations that could be easily solved, but the trouble is that the solution is not computed on the grid nodes, indeed we have

$$f_k(x - \lambda_k(t - t_n), t_n).$$

Hence, we should do an interpolation in order to project the exact solution on the grid. This problem can be avoided using a numerical scheme (such as the upwind scheme that is the less viscous one) to solve the equations, thus obtaining

$$f_{\varepsilon,k}^{m,n+1/2}.$$

Then we need to add the collision term, namely $\frac{1}{\varepsilon}(M_k(u) - f_k)$ to the omogeneous equations. To this aim we introduce

$$\tilde{f}_k' = \frac{1}{\varepsilon}(M_k(\sum_l \tilde{f}_l) - \tilde{f}_k),$$

with $\tilde{f}_k(t_n) = f_{\varepsilon,k}^{m,n+1/2}$. It is easy to verify that the function $\tilde{f}$ satisfies suitable compatibility conditions, see [9].

$$\left(\sum_k \tilde{f}_k\right)' = 0,$$

$$\sum_k \tilde{f}_k = \sum_k f_{\varepsilon,k}^{m,n+1/2} = u_\varepsilon^{m,n+1/2}.$$

Now we can compute the exact solution

$$f_{\varepsilon,k}^{n+1} = \tilde{f}_k(t^{n+1}) = M_k(u_\varepsilon^{m,n+1/2}) + e^{-\frac{\Delta t}{\varepsilon}}(\tilde{f}_k(t^n) - M_k(u_\varepsilon^{m,n+1/2})) \tag{2.3}$$

and write the scheme in the following form

$$\begin{aligned} f^{n+1/2} &= H_1(\Delta t) f^n, \\ f^{n+1} &= H_2(\Delta t) f^{n+1/2}, \end{aligned}$$

where H_1 is any scheme that discretizes the omogeneous equation and H_2 is as in (2.3). We fix $\varepsilon = 0$, thus obtaining the relaxed scheme, which can be written as

$$\begin{aligned} f^{n+1/2} &= H_1(\Delta t) f^n, \\ u^{n+1} &= u^{n+1/2} = \textstyle\sum_k f_k^{n+1/2}, \\ f^{n+1} &= M(u^{n+1}). \end{aligned}$$

We obtain an approximation of

$$u_t + F(u)_x = 0 \quad \text{in } \mathbb{R} \times (0, \infty), \tag{2.4}$$

$$u(x, 0) = u_0(x) \quad \text{on } \mathbb{R} \times \{t = 0\}, \tag{2.5}$$

which is stable, consistent and in conservation form,

$$u_m^{n+1} = u_m^n - \frac{\Delta t}{\Delta x}[\mathcal{F}_{m+1/2}^n - \mathcal{F}_{m-1/2}^n], \quad \forall m \geq 0,$$

where $\mathcal{F}^n_{m+1/2}$ is consistent with $F(u)$. One has

$$\mathcal{F}^n_{m+1/2} = \sum_k \lambda_k g^n_{m+1/2,k}(M_k(u^n_{m-k+1}), \ldots, M_k(u^n_{m+k}))$$

where g is the numerical flux of the linear equations. In microscopic variables the scheme reads

$$f_k^{m,n+1/2} = f_k^{m,n} - \lambda_k \frac{\Delta t}{\Delta x}(g^n_{m+1/2,k}(f^n_\varepsilon) - g^n_{m-1/2,k}(f^n_\varepsilon))$$

and the accuracy of the method depends on choice of the approximation scheme H_1. More general schemes have been proposed in [2].

2.0.3. *Discrete kinetic method for a boundary value problem.*
Here we present the discrete kinetic scheme for conservation laws. This method is a numerical approximation of the initial-boundary value problem for the one-dimensional conservation law:

$$u_t + F(u)_x = 0, \tag{2.6}$$

with initial data

$$u(x,0) = u_0(x), \quad x \geq 0 \tag{2.7}$$

and boundary data:

$$u(0,t) = u_b(t), \quad t \geq 0, \tag{2.8}$$

which can be imposed only where it is compatible with the trace of the solution to the problem and with the flux F. We have $u(x,t) \in \mathbb{R}^p$ ($p = 1$ in the scalar case) for $x \geq 0$, $t \geq 0$, and F is a Lipschitz continuous function.
These schemes are based on a kinetic approximation of the problem (2.6)-(2.7)-(2.8). Instead of solving (2.6), we solve the following BGK-like system of N non-linear equations in the unknowns $f^\varepsilon_k(x,t)$, $k = 1, \ldots, N$:

$$\partial_t f^\varepsilon_k + \lambda_k \partial_x f^\varepsilon_k = \frac{1}{\varepsilon}\Big(M_k(u^\varepsilon) - f^\varepsilon_k\Big), \tag{2.9}$$

where the λ_k are fixed velocities (a set of real numbers not all zero), ϵ is a positive parameter. Each f^ϵ_k is a function of $\mathbb{R}^+ \times [0,T]$ and takes values in $\mathbb{R}$. We impose the corresponding initial and boundary data:

$$f^\epsilon_k(x,0) = M_k(u_0(x)), \quad x \in \mathbb{R}^+, \tag{2.10}$$

$$f^\epsilon_k(0,t) = M_k(u_b(t)) \quad \forall\ \lambda_k > 0 \text{ and } t \geq 0. \tag{2.11}$$

Functions M_k, $k = 1, \ldots, N$, are the Maxwellian functions depending on u^ϵ, F and λ_i. To have the convergence of $u^\varepsilon = \sum_{k=1}^N f^\varepsilon_k$ $\varepsilon \to 0$ towards the solution of the problem (2.6), we need to recall the following compatibility conditions

$$\sum_{k=1}^N M_k(u) = u, \qquad \sum_{k=1}^N \lambda_k M_k(u) = F(u), \tag{2.12}$$

that show the link between problem (2.6)-(2.7)-(2.8) and system (2.9).

Definition 2.1
The function M is Monotone Non Decreasing (MND) on I, if $M_k'(u) \geq 0$ for $k \in \{1, \ldots, N\}$ and all $u \in I$.

If M is MND on I, then the following condition is satisfied for all $u \in I$:

$$\min_k \lambda_k \leq F'(u) \leq \max_k \lambda_k, \tag{2.13}$$

that is a subcharacteristic condition for the relaxation problem. The fact that M is MND is a sufficient condition for convergence, because it is related to the stability of the method.

2.0.4. *Numerical scheme.* We discretize the problem (2.9)-(2.10)-(2.11) and making ϵ tend to zero, we obtain a numerical scheme for the initial boundary value problem for the conservation law (2.6). For the convergence results for the discrete kinetic appoximation for conservation laws, without considering the problem at the junctions, see [1].
The data of the problem are approximated by

$$\begin{aligned} u_b^n &= u_{-1}^n = \frac{1}{\Delta t}\int_{t_n}^{t_{n+1}} u_b(t)dt, \quad 0 \leq n \leq M-1, \\ u_m^0 &= \frac{1}{\Delta x}\int_{x_{m-\frac{1}{2}}}^{x_{m+\frac{1}{2}}} u^0(x)dx, \quad m \in \mathbb{N}, \end{aligned}$$

and we take for all k:

$$\begin{aligned} f_{-1,k}^n &= M_k(u_b^n), \quad 0 \leq n \leq M-1, \\ f_{m,k}^0 &= M_k(u_m^0), \quad m \in \mathbb{N}. \end{aligned}$$

2.0.5. *First order in time discretization.* We split the operators used to solve system (2.9) into two parts: the *transport* part and the *collision* part.

Transport:
the set of transport equations discretized on $[t_n, t_{n+1}]$:

$$\begin{cases} \partial_t f_k^{m,n} + \lambda_k \partial_x f_k^{m,n} = 0, & k = 1, \ldots, N, \\ f(x, t_n) = f_\Delta^n(x), & \\ f_k(0,t) = f_{b,k}^n & \text{if } \lambda_k > 0. \end{cases}$$

The scheme can be written in conservation form for all $i \geq 0$:

$$f_{m,k}^{n+\frac{1}{2}} = f_{m,k}^n - \lambda_k \frac{\Delta t}{\Delta x}(f_{m+\frac{1}{2}}^n - f_{m-\frac{1}{2}}^n), \quad k \in \{1, \ldots, N\}. \tag{2.14}$$

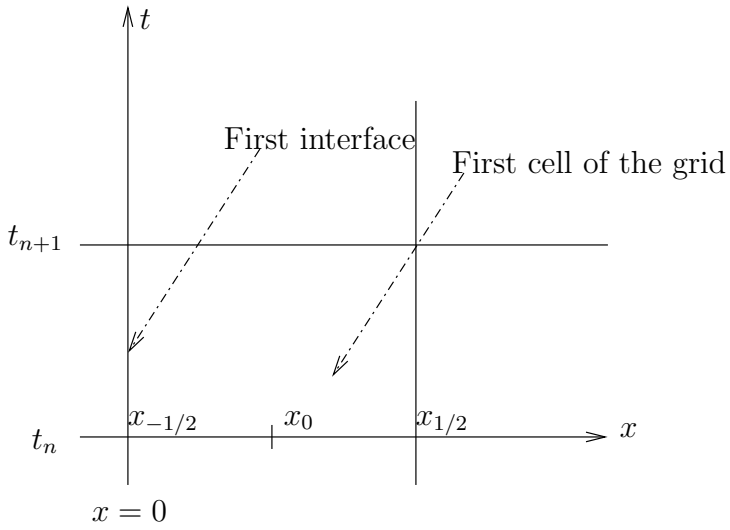

FIGURE 2. The grid at the boundary.

The numerical flux, namely $\lambda_k f^n_{m+\frac{1}{2}}$, is a Lipschitz continuous function $\lambda_k \mathcal{F}_k$ depending on $\{f^n_{m+l,k}, -1 \leq l \leq 2\}$ and it verifies the consistency condition

$$\mathcal{F}(f, \ldots, f) = f. \tag{2.15}$$

The scheme, written in the Harten formulation including both first and second order in space approximation, reads

(2.16)

$$i \geq 0, \begin{cases} f^{n+\frac{1}{2}}_{m,k} = f^n_{m,k}(1 - D^n_{m-\frac{1}{2},k}) + D^n_{m-\frac{1}{2},k} f^n_{m-1,k}, & \text{if } \lambda_k > 0, \\ f^{n+\frac{1}{2}}_{m,k} = f^n_{m,k}(1 - D^n_{m+\frac{1}{2},k}) + D^n_{m+\frac{1}{2},k} f^n_{m+1,k}, & \text{if } \lambda_k \leq 0. \end{cases}$$

Note that it is necessary to assign the boundary value $f^n_{b,k} = f^n_{-1,k}$ only for positive velocities.

Remark 2.2 At first order the upwind approximation is chosen:

$$D^n_{m-\frac{1}{2},k} = D^n_{m+\frac{1}{2},k} = \xi_k = |\lambda_k| \frac{\Delta t}{\Delta x}$$

and in that case (2.16) is well defined even for $i = 0$.

■

At higher order, $D^n_{m+\frac{1}{2},k}$ is a nonlinear function and we introduce it in the next subsection.
In all cases the time step restriction is

$$\max_{1 \leq k \leq N} |\lambda_k| \Delta t \leq \Delta x. \tag{2.17}$$

Collision:

Now we use the solution obtained for the precedent scheme as the initial condition for the ODS on $[t_n, t_{n+1}]$:

$$\begin{cases} \partial_t f_k^{m,n} = \frac{1}{\epsilon}(M_k(u) - f_k(t)), & k = 1, \dots, N, \\ f_k(0) = f(0), \quad x \geq 0. \end{cases}$$

Under the compatibility conditions (2.12) we are able to solve exactly the differential system. The solution, for ϵ fixed, can be written as

(2.18)
$$f_{m,k}(t_{n+1}) = (1 - e^{-\frac{\Delta t}{\epsilon}})M_k(u_m^{n+\frac{1}{2}}) + e^{-\frac{\Delta t}{\epsilon}} f_{m,k}^{n+\frac{1}{2}}, \quad m \geq 0, \quad n \geq 1.$$

The identity holds

$$u_m^{n+1} = \sum_k f_{m,k}^{n+\frac{1}{2}} = u_m^{n+\frac{1}{2}}. \tag{2.19}$$

When $\epsilon \to 0$, the projection reads

$$f_{m,k}^{n+1} = M_k(u_m^{n+\frac{1}{2}}) = M_k(u_m^{n+1}), \quad m \geq 0, \quad n \geq 1. \tag{2.20}$$

Now that we have completely described a whole time step, we present the scheme in macroscopic variables:

$$u_m^{n+1} = u_m^n - \frac{\Delta t}{\Delta x}(g_{m+1/2}^n - g_{m-1/2}^n), \tag{2.21}$$

where

$$g_{m+1/2}^n = \sum_{k=1}^N \lambda_k f_{m+\frac{1}{2},k}^n, \quad m \geq 0.$$

This scheme is consistent since

$$g_{m+1/2}^n = \mathcal{G}(u_{m-1}^n, \dots, u_{m+2}^n) = \sum_{k=1}^N \lambda_k \mathcal{F}_k(M_k(u_{m-1}^n), \dots, M_k(u_{m+2}^n))$$

and, due to conditions (2.12) and (2.15):

$$\mathcal{G}(u, \dots, u) = F(u).$$

If we use the upwind first order method to approximate the transport part, the numerical flux can be written in the following form:

$$g_{m+1/2}^n = \sum_{\lambda_k > 0} \lambda_k M_k(u_m^n) + \sum_{\lambda_k < 0} \lambda_k M_k(u_{m+1}^n),$$

$$g_{m-1/2}^n = \sum_{\lambda_k > 0} \lambda_k M_k(u_{m-1}^n) + \sum_{\lambda_k < 0} \lambda_k M_k(u_m^n).$$

We suppose that the Maxwellian functions are MND, so we have the usual CFL condition

$$\max_u |F'(u)| \Delta t \leq \Delta x$$

and, from the transport part of the scheme, we have to impose the time step restriction in (2.17).

2.0.6. *Boundary condition.* In macroscopic variables, the flux on the boundary interface reads:

$$g^n_{-1/2} = \sum_{\lambda_k>0} \lambda_k M_k(u^n_b) + \sum_{\lambda_k<0} \lambda_k M_k(u^n_0).$$

Notice that there is no need of ghost cells and that we use the same scheme on the whole grid. To compute the approximated solution for $m = N$, it is necessary to know the value u^n_{N+1}, that can be obtained imposing a Neumann condition.

2.0.7. *Conditions at a junction.* For roads entering the junction we invert the flux function f following the rule:

- if $u^n_N \in [0, \sigma]$ and $\hat{\gamma}_i < F(u^n_N)$ then $F^{-1}(\hat{\gamma}_i) \in [\tau(u^n_N), 1)$,
- if $u^n_N \in [0, \sigma]$ and $\hat{\gamma}_i = F(u^n_N)$ then $F^{-1}(\hat{\gamma}_i) = u^n_N$,
- if $u^n_N \in [\sigma, 1]$ then $F^{-1}(\hat{\gamma}_i) \in [\sigma, 1]$,

with $i = 1, 2$.
For roads coming out of the junction we invert the flux function with the rule

- if $u^n_0 \in [\sigma, 1]$ and $\hat{\gamma}_j < F(u^n_0)$ then $F^{-1}(\hat{\gamma}_j) \in [0, \tau(u^n_0))$,
- if $u^n_0 \in [\sigma, 1]$ and $\hat{\gamma}_j = F(u^n_0)$ then $F^{-1}(\hat{\gamma}_j) = u^n_0$,
- if $u^n_0 \in [0, \sigma]$ then $f^{-1}(\hat{\gamma}_j) \in [0, \sigma]$,

with $j = 1, 2$.
At the right boundary ($m = N$) of roads linked to the junction on the right endpoint we set

$$u^{n+1}_N = u^n_N - \frac{\Delta t}{\Delta x}[g(u^n_N, F^{-1}(\hat{\gamma}_i)) - g(u^n_{N-1}, u^n_N)],$$

while, for roads connected to a junction at the left endpoint one has:

$$u^{n+1}_0 = u^n_0 - \frac{\Delta t}{\Delta x}[g(u^n_0, u^n_1) - g(F^{-1}(\hat{\gamma}_j), u^n_0)].$$

2.0.8. *Second order in space.* The transport part can be approximated by a second order scheme as follows. Starting from $f^n_{i,k}$ we build a piecewise linear function:

$$\bar{f}^n_{m,k}(x) = f^n_{m,k} + (x - x_m)\sigma^n_{m,k}, \quad x \in (x_{m-\frac{1}{2}}, x_{m+\frac{1}{2}}),$$

where $\sigma^n_{m,k}$ are limited slopes and we solve exactly the transport equations on $[t_n, t_{n+1}]$. With the projection of the solution on the set of piecewise constant functions on the cells, we have for $\lambda_k > 0$:
(2.22)

$$f^{n+\frac{1}{2}}_{m,k} = f^n_{m,k}(1 - \xi_k) + \xi_k f^n_{m-1,k} - \frac{\xi_k(1 - \xi_k)}{2}(\sigma^n_{m,k} - \sigma^n_{m-1,k}), \quad m \geq 1.$$

For $\lambda_k \leq 0$:
(2.23)
$$f^{n+\frac{1}{2}}_{m,k} = f^n_{m,k}(1-\xi_k) + \xi_k f^n_{m+1,k} - \frac{\xi_k(1-\xi_k)}{2}(\sigma^n_{m+1,k} - \sigma^n_{m,k}), \quad m \geq 0,$$

so we obtain the explicit expression for $D^n_{m+\frac{1}{2},k}$:

$$D^n_{m+\frac{1}{2},k} = \xi_k \left(1 + sgn(\lambda_k)\Delta x \frac{(1-\xi_k)}{2} \frac{(\sigma^n_{m+1,k} - \sigma^n_{m,k})}{\Delta f^n_{m+\frac{1}{2},k}}\right), \tag{2.24}$$

with the convention that if $\Delta f^n_{m+\frac{1}{2},k} = 0$, then $D^n_{m+\frac{1}{2},k} = \xi_k = |\lambda_k|\frac{\Delta t}{\Delta x}$. Note that if $\lambda_k > 0$ (2.24) is defined for $m \geq -1$, in the other cases is available for $m \geq 0$. The slopes $\sigma^n_{m,k}$ are defined for $m \geq 1$ as:

$$\sigma^n_{m,k} = minmod\left(X^1_{m,k}\frac{\Delta f^n_{m+\frac{1}{2},k}}{\Delta x}, X^2_{m,k}\frac{\Delta f^n_{m-\frac{1}{2},k}}{\Delta x}\right),$$

with

$$\Delta f^n_{m+\frac{1}{2},k} = f^n_{m+1,k} - f^n_{m,k}$$

and

$$minmod(a,b) = \min(|a|,|b|)\frac{sgn(a)+sgn(b)}{2}.$$

The amplifying coefficients $X^1_{m,k}$, $X^2_{m,k}$ can be taken to make the upwind scheme closer to the central scheme, without loss of stability. In this case we choose $X^1_{m,k} = X^2_{m,k} = 1$.

2.0.9. *Boundary conditions.* For $m = 0$ we take for the boundary

$$\sigma^n_{-1,k} = 0,$$

so that (2.22) still holds for $m = 0$. In this case, the slope $\sigma^n_{0,k}$ can be defined as

- for $\lambda_k > 0$:

  $$\sigma^n_{0,k} = minmod\left(X^1_{0,k}\frac{f^n_{1,k} - f^n_{0,k}}{\Delta x}, 2X^2_{0,k}\frac{f^n_{0,k} - M_k(u^n_b)}{\Delta x}\right),$$

  where u^n_b is the boundary condition;
- for $\lambda_k < 0$:

  $$\sigma^n_{0,k} = X^1_{0,k}(f^n_{1,k} - f^n_{0,k}).$$

When $m = N$ the scheme for $\lambda_k < 0$ requires the values $f^n_{N+1,k}, f^n_{N+2,k}$, that can be obtained, for instance, imposing a Neumann condition.

2.0.10. *Conditions at a junction.* As usual, to impose the boundary condition at a junction we need to examine the links between the roads. The inversion of f is performed as explained before. At the right boundary ($m = N$) of roads linked to the junction on the right endpoint one has:

$$f_{N,k}^{n+\frac{1}{2}} = f_{N,k}^n(1 - D_{N+\frac{1}{2},k}^n) + D_{N+\frac{1}{2},k}^n f_{N+1,k}^n, \qquad \text{for } \lambda_k < 0,$$

with

$$f_{N+1,k}^n = M_k(f^{-1}(\hat{\gamma}_i)).$$

Due to the lack of a rigorous theory that allows to take second order boundary conditions up to the junctions, we set

- for $\lambda_k > 0$:
$$\sigma_{N,k}^n = 0,$$
- for $\lambda_k > 0$:
$$\sigma_{N,k}^n = 0,$$

thus reducing to a first order scheme at the junctions. Moreover we use the Neumann condition $f_{N+2,k}^n = f_{N+1,k}^n$.
At the left boundary ($m = 0$) of roads linked to the junction on the left endpoint the scheme in case $\lambda_k > 0$ reads:

$$f_{0,k}^{n+\frac{1}{2}} = f_{0,k}^n(1 - D_{-\frac{1}{2},k}^n) + D_{-\frac{1}{2},k}^n f_{-1,k}^n,$$

with

$$f_{-1,k}^n = M_k(f^{-1}(\hat{\gamma}_j)).$$

Due to the lack of a rigorous theory that allows to take second order boundary conditions up to the junctions, we set

- for $\lambda_k > 0$:
$$\sigma_{-1,k}^n = 0, \quad \sigma_{0,k}^n = 0,$$
- for $\lambda_k <= 0$:
$$\sigma_{0,k}^n = 0,$$

thus reducing to a first order scheme at the junctions.

2.0.11. *Discrete kinetic models.* Here follows a presentation of the different approximations we used in kinetic schemes.

- **Two velocities model.** $N = 2$, $\lambda_1 = -\lambda_2 = -\lambda$. We approximate the scalar conservation law

$$\partial_t \rho + \partial_x f(\rho) = 0 \tag{2.25}$$

by the relaxation system

$$\begin{cases} \partial_t u + \partial_x v = 0, \\ \partial_t v + \lambda^2 \partial_x u = \frac{1}{\varepsilon}(F(u) - v), \end{cases} \tag{2.26}$$

which is diagonalized in the form

$$\begin{cases} \partial_t f_1^\varepsilon - \lambda \partial_x f_1^\varepsilon = \frac{1}{\varepsilon}(M_1(u^\varepsilon) - f_1^\varepsilon), \\ \partial_t f_2^\varepsilon + \lambda \partial_x f_2^\varepsilon = \frac{1}{\varepsilon}(M_2(u^\varepsilon) - f_2^\varepsilon) \end{cases}$$

and the associated Maxwellian functions are

$$M_1(u) = \frac{1}{2}\left(u - \frac{F(u)}{\lambda}\right),$$

$$M_2(u) = \frac{1}{2}\left(u + \frac{F(u)}{\lambda}\right).$$

In order to respect the monotonicity condition MND on $I \subset \mathbb{R}$, the derivatives must satisfy

$$M'_{1,2} = \frac{1}{2}\left(1 \pm \frac{A'(u)}{\lambda}\right) \geq 0, \forall u \in I,$$

that gives the following condition on the velocity vector λ:

$$\max_{u\in I} |F'(u)| < \lambda, \tag{2.27}$$

which is the scalar version of the subcharacteristic condition. For the relaxation system (2.26) there is a freedom degree while imposing the boundary condition that reads

$$f_2(0,t) = M_2(u_b(t)) - \alpha(f_1(0,t) - M_1(u_b(t))), \tag{2.28}$$

with $\alpha \in [-1,1]$. Condition (2.28) can be written in a discrete form as

$$f_2(0,t) = M_2(u_b^n) - \alpha(f_{0,1}^n - M_1(u_b^n)).$$

Note that for $\alpha = 0$ we have the equilibrium on f_2. The first order discretization of this model gives a Lax-Friedrichs type scheme.

- **Three velocities model.** Dealing with more velocities corresponds to more accurate approximation schemes. Take $N = 3$ and the velocities $\lambda_3 = -\lambda_1 = \lambda > 0$, $\lambda_2 = 0$. The approximation kinetic system is

$$\begin{cases} \partial_t f_1^\varepsilon - \lambda \partial_x f_1^\varepsilon = \frac{1}{\varepsilon}(M_1(u^\varepsilon) - f_1^\varepsilon), \\ \partial_t f_2^\varepsilon = \frac{1}{\varepsilon}(M_2(u^\varepsilon) - f_2^\varepsilon), \\ \partial_t f_3^\varepsilon + \lambda \partial_x f_3^\varepsilon = \frac{1}{\varepsilon}(M_3(u^\varepsilon) - f_3^\varepsilon), \end{cases}$$

with the Maxwellian functions given by

$$M_1(u) = \frac{1}{\lambda}\begin{cases} 0, & \text{if } u \leq \frac{1}{2}, \\ u(u-1) + \frac{1}{4}, & \text{if } u \geq \frac{1}{2}, \end{cases}$$

$$M_2(u) = \begin{cases} \left(1 - \frac{1}{\lambda}\right) u + \frac{1}{\lambda}u^2, & \text{if } u \leq \frac{1}{2}, \\ \left(1 + \frac{1}{\lambda}\right) u - \frac{1}{\lambda}u^2 - \frac{1}{2\lambda}, & \text{if } u \geq \frac{1}{2}, \end{cases}$$

$$M_3(u) = \frac{1}{\lambda}\begin{cases} u(1-u), & \text{if } u \leq \frac{1}{2}, \\ \frac{1}{4}, & \text{if } u \geq \frac{1}{2}. \end{cases}$$

At the boundary we impose

$$f_3(0,t) = M_3(u_b(t))$$

and the Maxwellian are MND if and only if the condition (2.27) is satisfied. In this case (2.27) reads

$$0 \leq M_2'(u) \leq 1 - \frac{|F'(u)|}{\lambda}.$$

This model, at first order, is the kinetic expression of the Engquist-Osher scheme. All of these schemes have been already proposed in [10].

3. Numerical results

In this Section we present some numerical tests performed with the schemes precedently introduced, such as the Godunov's scheme (G), the three-velocities kinetic scheme of first order ($3VK_1$) and the three-velocities Kinetic method ($3VK_2$) with $\lambda_3 = -\lambda_1 = 1.0$ and $\lambda_2 = 0$. In general the three-velocities kinetic models work better than the two-velocities ones. We introduce the order γ of a numerical method in the following way:

$$\gamma = \log_2 \left(\frac{TOT_{err}(1)}{TOT_{err}(2)} \right), \tag{3.1}$$

where we define

$$e_p^r = \frac{h}{p} \frac{\sum_{j=0,\dots,N} \left| w_j^M \left(\frac{h}{p} \right) - w_j^M \left(\frac{h}{2p} \right) \right|}{\sum_{j=0,\dots,N} \left| w_j^M \left(\frac{h}{p} \right) \right|}, \quad p = 1, 2, r = 1, \dots, S. \tag{3.2}$$

The quantity S indicates the number of the roads in the network and $w_m^M(h)$ denotes the numerical solution obtained with the space step discretization equal to h, calculated in x_m at the final time $t_M = T$. Then the total error is

$$TOT_{err}(p) = \sum_{r=1}^{S} e_p^r, \quad p = 1, 2. \tag{3.3}$$

Here we present some numerical tests for traffic lights.
First we consider a road parametrized by the interval $[0, 2]$, with a traffic light in correspondence of $x_L = 1.0$.

3.1. **Traffic lights.** Before showing the numerical experiments on the traffic light, we need to introduce the suitable boundary conditions for the numerical schemes at x_L.

3.1.1. *Conditions at the traffic light.* Let $m = m_L$ be the node of the numerical mesh of the discretization corresponding to the point where is placed the traffic light.
Consider first the Godunov's method. For the space node on the left of the traffic light we set

$$v_{m_L-1}^{n+1} = v_{m_L-1}^n - \frac{\Delta t}{\Delta x}(g^G(v_{m_L-1}^n, 1) - g^G(v_{m_L-2}^n, v_{m_L-1}^n)), \tag{3.4}$$

while for the node on the right we have

$$v_{m_L}^{n+1} = v_{m_L}^n - \frac{\Delta t}{\Delta x}(g^G(v_{m_L}^n, v_{m_L+1}^n) - g^G(0, v_{m_L}^n)). \tag{3.5}$$

Notice that for the relaxation scheme written in the macroscopic variables the conditions at the traffic lights coincide with the conditions written for the Godunov's method.
Let us now turn to the kinetic scheme written in the microscopic variables. At the left boundary respect to the traffic light ($m = m_L - 1$) the scheme reads:
(3.6)

$$f_{m_L-1,k}^{n+\frac{1}{2}} = f_{m_L-1,k}^n(1 - D_{m_L-1+\frac{1}{2},k}^n) + D_{m_L-1+\frac{1}{2},k}^n f_{m_L,k}^n, \quad \text{for } \lambda_k <= 0,$$

where we set

$$f_{m_L,k}^n = M_k(1).$$

For $\lambda_k <= 0$ we have

$$\sigma_{m_L-1,k}^n = minmod\left(2\frac{f_{m_L,k}^n - f_{m_L-1,k}^n}{\Delta x}, \frac{f_{m_L-1,k}^n - f_{m_L-2,k}^n}{\Delta x}\right), \quad \sigma_{m_L,k}^n = 0,$$

and in the case $\lambda_k > 0$ we set

$$\sigma_{m_L-1,k}^n = f_{m_L-1,k}^n - f_{m_L-2,k}^n.$$

At the right boundary ($m = m_L$) the scheme is

$$f_{m_L,k}^{n+\frac{1}{2}} = f_{m_L,k}^n(1 - D_{m_L-\frac{1}{2},k}^n) + D_{m_L-\frac{1}{2},k}^n\ f_{m_L-1,k}^n, \quad \text{for } \lambda_k > 0, \tag{3.7}$$

where we set

$$f_{m_L-1,k}^n = M_k(0).$$

For $\lambda_k > 0$ we have

$$\sigma_{m_L-1,k}^n = 0, \quad \sigma_{m_L,k}^n = minmod\left(\frac{f_{m_L+1,k}^n - f_{m_L,k}^n}{\Delta x}, 2\frac{f_{m_L,k}^n - f_{m_L-1,k}^n}{\Delta x}\right),$$

and in the case $\lambda_k <= 0$ we have

$$\sigma_{m_L,k}^n = f_{m_L+1,k}^n - f_{m_L,k}^n.$$

At $t = 0$ the light is assumed to be red and, for simplicity, we fix $\Delta_g = \Delta_r = 1.0$ (recall the definitions given in the description of the model at a junction.
Let us assume on the road the following initial and boundary data:

$$\begin{aligned} \rho(x, 0) &= 0.3, \\ \rho_b(t) &= 0.5. \end{aligned} \tag{3.8}$$

The approximated solutions are computed by three methods, such as Godunov's scheme (G), three velocities kinetic method of first order ($3VK_1$) and 3 velocities kinetic method of second order ($3VK_2$).
At $t = 0$ the light is red, thus the density becomes high at $x = 1.0$ where the traffic light is placed and there is the generation of a shock propagating backwards, see Figure 3.
After the light turns green, cars can go, corresponding to the creation of a rarefaction wave in the direction of traffic flow, as showed in Figure 4. When the light becomes red, it is produced again a shock in correspondence of the point where is placed the traffic light, see Figure 5 and after a short time, we can observe a big value of the car density at the entrance of the road, as depicted in Figure 6. Considering again the data (3.8) and taking $\Delta_g = 1.5$ and $\Delta_r = 0.5$, thus meaning that the time of green is three times the time of red, one can see that at time $T = 3.8$ the value of density is much lower than in precedence, as showed by Figure 7.

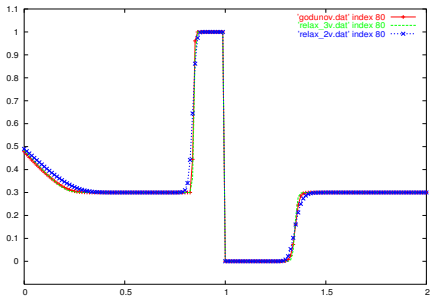

FIGURE 3. Density when the light is red, $h = 0.0125$, $T = 0.5$.

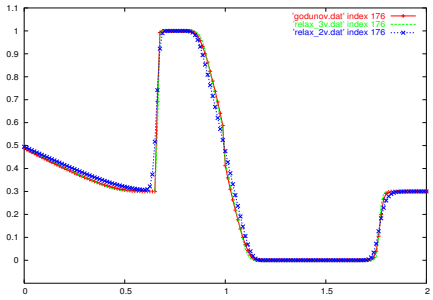

FIGURE 4. Density after the light turns green, $h = 0.0125$, $T = 1.1$.

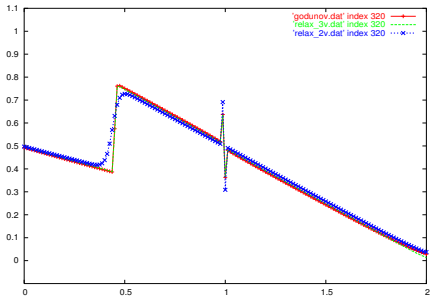

FIGURE 5. The light is again red, high density at $x = 1$, $h = 0.0125$, $T = 2.0$.

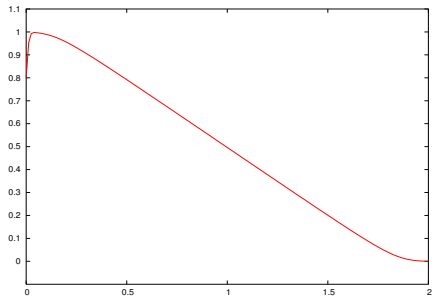

FIGURE 6. High density at the entrance ($x = 0$), $\Delta_g = \Delta_r = 1.0$, $h = 0.0125$, $T = 3.8$.

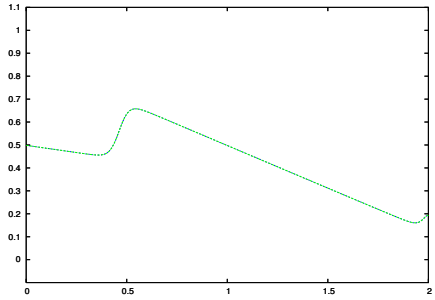

FIGURE 7. Traffic can still enter on the left, $h = 0.0125$, $\Delta_g = 1.5$, $\Delta_r = 0.5$, $T = 3.8$.

In the next table are reported order and errors for the approximated solution computed with the following methods, such as the Godunov's scheme (G), 3 velocities Kinetic method of first order ($3VK_1$) and 3 velocities Kinetic method of second order ($3VK_2$). The initial and boundary data are (3.8) and we set $\Delta_g = \Delta_r = 1.0$.

	G		$3VK_1$		$3VK_2$	
h	γ	L^1 Error	γ	L^1 Error	γ	L^1 Error
0.1	1.074739	0.048958	1.098426	0.050723	1.518485	0.026815
0.05	0.717578	0.023243	0.740926	0.023689	1.584962	0.009360
0.025	0.732966	0.014135	0.738094	0.014174	1.608739	0.003120
0.0125	0.743919	0.008504	0.741168	0.008498	1.584962	0.001057
0.00625	0.779725	0.005078	0.764019	0.005084	1.560714	0.000341
0.003125	0.840073	0.002958	0.829557	0.002994	1.580145	0.000114

TABLE TL1 Convergence order γ, defined in (3.1), and errors of the approximation schemes Godunov (G), 3 velocities Kinetic methods of first order ($3VK_1$) and of second order ($3VK_2$) for data 3.8, $\Delta_g = \Delta_r = 1.0$,

$T = 2$.

From this simple example it is easy to see that tuning the values Δ_g, Δ_r it is possible to control traffic.

3.2. **Junction with 2 outgoing and 2 incoming roads.** Recall definitions given in the description of the model of a junction J with two incoming roads and two outgoing roads all parametrized by the intervals $[0,1]$. Here we refer to the situation described in Appendix of [4], where the coefficients of the distribution matrix A are such that $0 < \alpha_{32} < \alpha_{31} < 1/2$ and we set

$$\alpha_{31} = \alpha_1, \quad \alpha_{32} = \alpha_2, \quad \alpha_{41} = 1 - \alpha_1, \quad \alpha_{42} = 1 - \alpha_2$$

and we introduce the notation

$$\rho_1(x,0) = \rho_{1,0}, \quad \rho_2(x,0) = \rho_{2,0}, \quad \rho_3(x,0) = \rho_{3,0}, \quad \rho_4(x,0) = \rho_{4,0}.$$

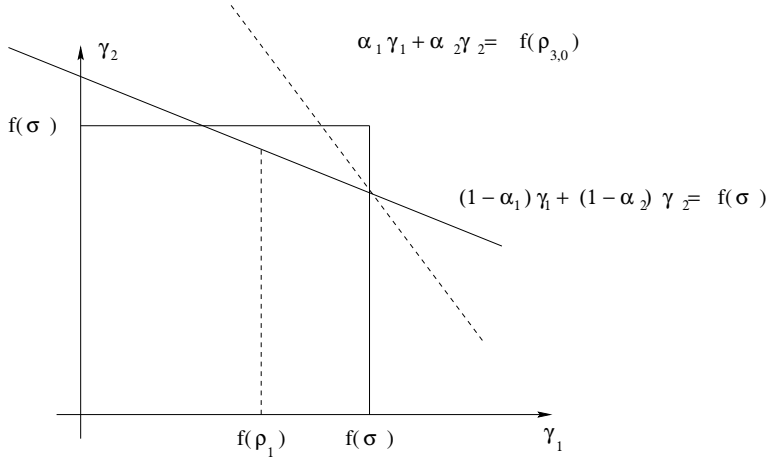

FIGURE 8. Solution to the Riemann's problem at J.

The distribution matrix is fixed as follows

$$A = \begin{pmatrix} 0.4 & 0.3 \\ 0.6 & 0.7 \end{pmatrix} \tag{3.9}$$

and we consider the following constant initial and boundary data

$$\rho_{1,0} = \rho_{4,0} = \sigma, \qquad \rho_{2,0} = \rho_{3,0} = f^{-1}\left(\frac{\alpha_1}{1-\alpha_2} f(\sigma)\right) = 0.82732683535,$$

$$\rho_{1,b}(t) = \sigma, \qquad \rho_{2,b}(0,t) = f^{-1}\left(\frac{\alpha_1}{1-\alpha_2} f(\sigma)\right) = 0.82732683535\ . \tag{3.10}$$

Remark 3.1 Notice that the boundary condition is imposed only on the incoming roads, as for the outgoing ones we use a Neumann condition at the final endpoint.

■

In the next figures we will use the following convention: road 1 is on the upper-left, road 3 is on the upper-right, road 2 on the lower left and road 4 on the lower right. The numerical solutions in the following figures have been produced with the Godunov's method.

Let us introduce a perturbation on the initial data of road 1

$$\rho_1(0,x) = \begin{cases} \rho_{1,0} = \sigma & \text{if } 0 \le x \le 0.5, \\ \rho_1 & \text{if } x \ge 0.5, \end{cases} \tag{3.11}$$

and $\rho_1,\ \rho_{1,0},\ \rho_{2,0},\ \rho_{3,0},\ \rho_{4,0}$ be constants such that

$$\sigma < \rho_{2,0} < 1, \quad \sigma < \rho_{3,0} < 1, \quad \rho_1 < \sigma, \quad \rho_{1,0} = \rho_{4,0} = \sigma, \tag{3.12}$$

$$f(\rho_{1,0}) = f(\rho_{4,0}) = f(\sigma), \quad f(\rho_{2,0}) = f(\rho_{3,0}) = \frac{\alpha_1}{1-\alpha_2} f(\sigma),$$

so that $(\rho_{1,0},\, \rho_{2,0},\, \rho_{3,0},\, \rho_{4,0})$ is an equilibrium configuration, see Figures 9, 10.

In (3.11) set $\rho_1 = 0.25$ and let $\rho_{1,b} = 0.25$ be the boundary data on road 1. We take $\rho_{2,0},\ \rho_{3,0},\ \rho_{4,0}$ as in (3.10) and the boundary data on road 2 is $\rho_{1,b} = \rho_{20}$. The initial configuration is depicted in Figure 11. After a certain time ($t = 3$) the wave $(\rho_1, \rho_{1,0})$ interacts with the junction, see Figure 12, and the situation at time $t = 38$ is described in Figure 13: road 2 and road 3 have to lower their flux, hence they produce waves moving with positive speed. At time $T = 80$ the new equilibrium configuration is reached, as showed by Figure 14.
Now, in (3.11) assume to have a smaller perturbation represented by $\rho_1 = 0.4$ and let the boundary data on road 1 be $\rho_{1,b} = 0.4$. The initial data on the other roads of the junction, namely $\rho_{2,0},\ \rho_{3,0},\ \rho_{4,0}$, are taken as in (3.10) and the boundary data on road 2 is $\rho_{1,b} = \rho_{20}$. The initial configuration is depicted in Figure 15.
After a certain time ($t = 10$) the wave $(\rho_1, \rho_{1,0})$ interacts with the junction, see Figure 16, and the situation at time $t = 75$ is described in Figure 17: road 2 and road 3 have to lower their flux, hence they produce a wave moving with positive speed. The wave generated on road 2 has a very little width. At time $T = 470$ the new equilibrium configuration is reached, as showed by Figure 18.

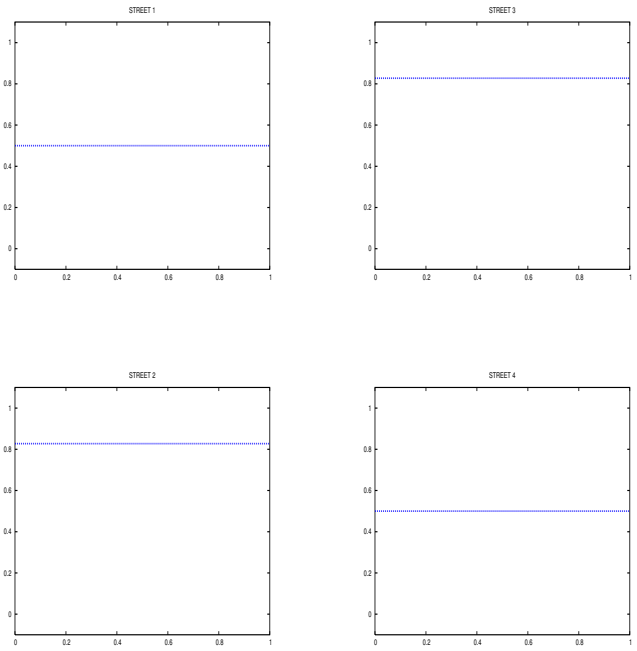

FIGURE 9. An equilibrium configuration, $h = 0.025, T = 0$.

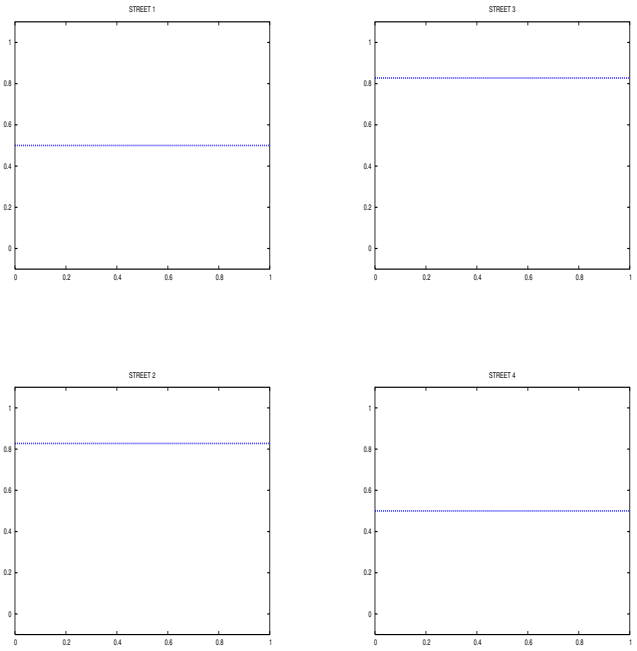

FIGURE 10. An equilibrium configuration, $h = 0.025, T = 10$.

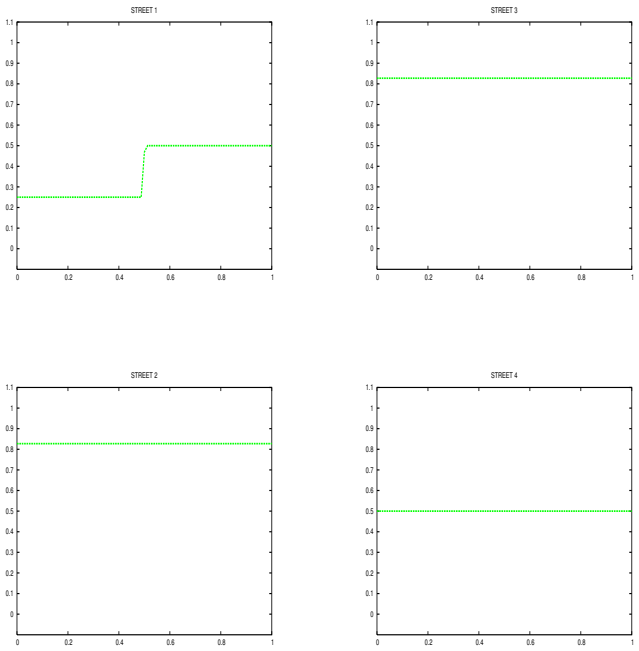

FIGURE 11. Perturbation on road 1, $h = 0.025, T = 0$.

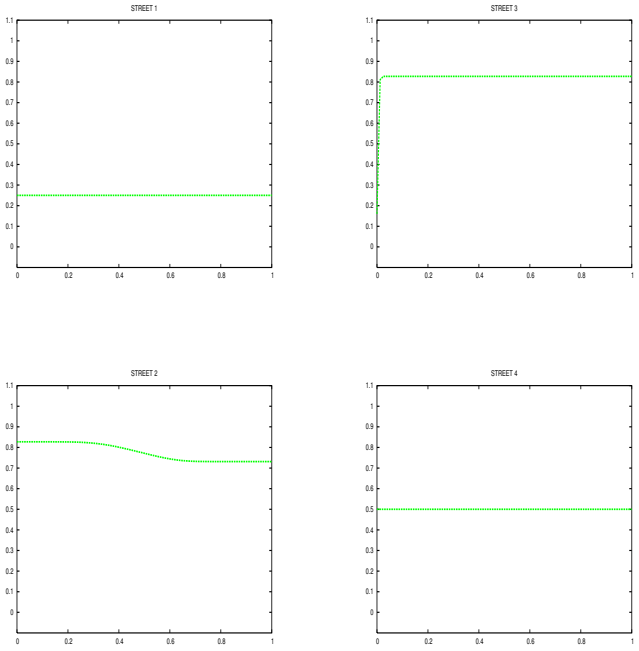

FIGURE 12. Perturbation on road 1 travels through the junction, producing a rarefaction waves travelling on roads 2 and 3, $h = 0.025, T = 3$.

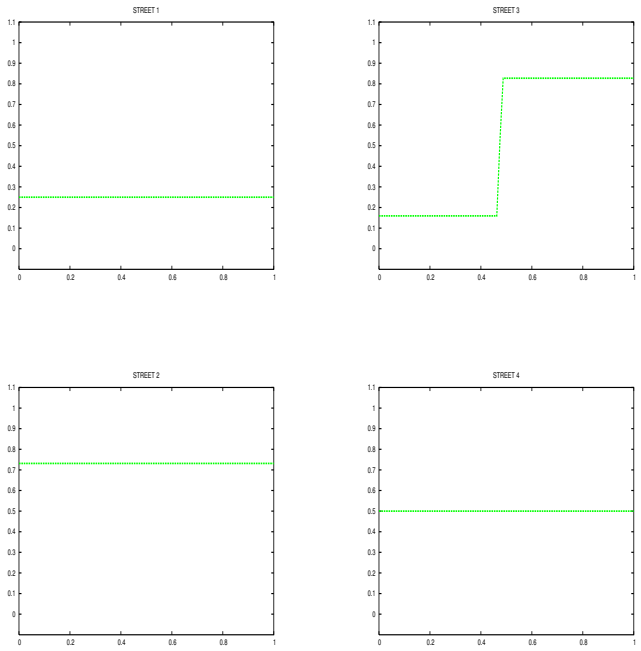

FIGURE 13. Perturbation on road 1 travels on roads 2 and 3, $h = 0.025, T = 38$.

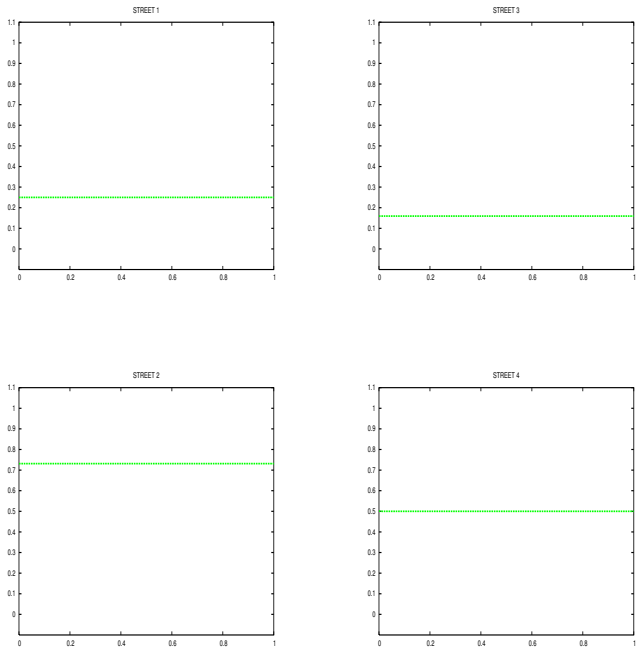

FIGURE 14. The new equilibrium configuration, $h = 0.025, T = 80$.

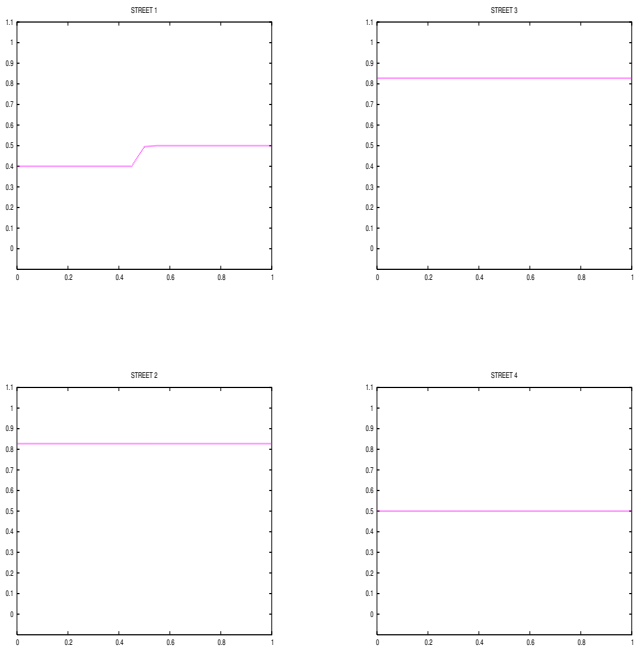

FIGURE 15. Perturbation on road 1, $h = 0.025, T = 0$.

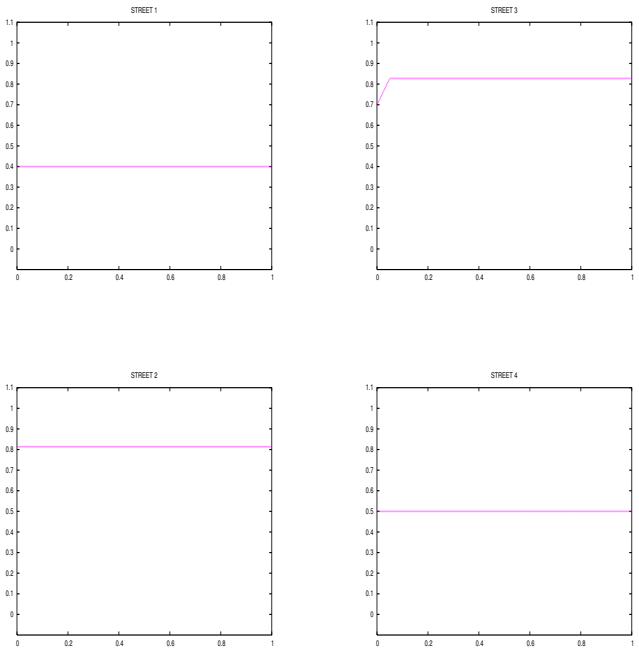

FIGURE 16. Perturbation on road 1 travels through the junction, $h = 0.025, T = 10$.

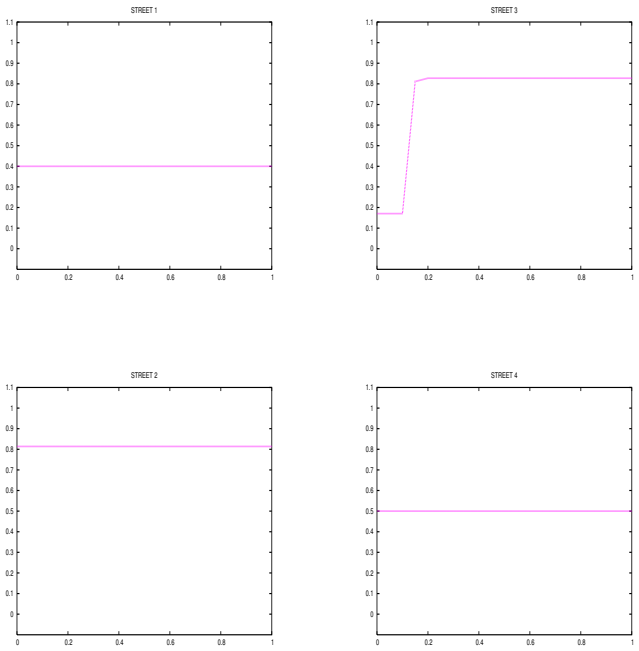

FIGURE 17. Perturbation on road 1 produces a rarefaction wave travelling on road 3, $h = 0.025, T = 75$.

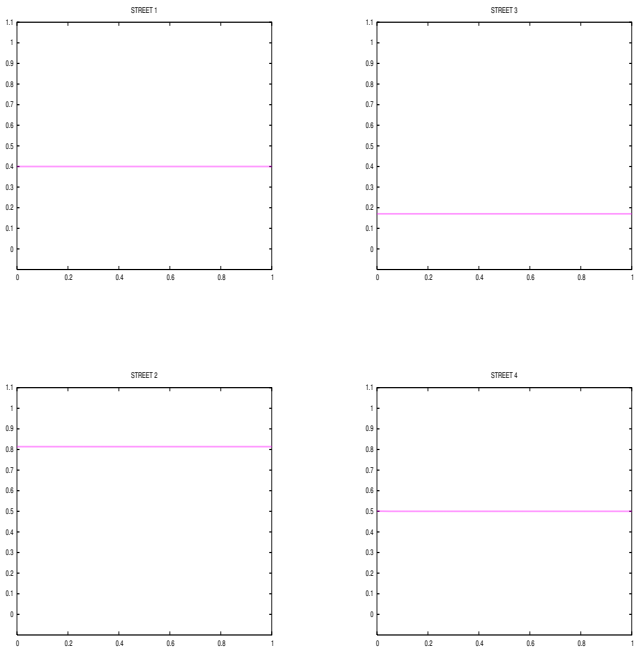

FIGURE 18. The new equilibrium configuration, $h = 0.025, T = 470$.

In the following table are reported orders and errors for the first test before the interaction.

	G		$3VK_1$		$3VK_2$	
h	γ	L^1 Error	γ	L^1 Error	γ	L^1 Error
0.1	0.827170	0.011818	0.8317251	0.009944	1.528182	0.009825
0.05	0.895236	0.006661	0.856393	0.006218	1.510920	0.004214
0.025	0.933869	0.003581	0.893219	0.004052	1.545241	0.000843
0.0125	0.956749	0.001875	0.948823	0.001145	1.554962	0.000438
0.00625	0.970390	0.000966	0.985218	0.000873	1.526867	0.00091
0.003125	0.997122	0.000493	1.017662	0.000461	1.507213	0.000242

TABLE Convergence order γ, defined in (3.1), and errors of the approximation schemes Godunov (G), 3 velocities Kinetic methods of first order ($3VK_1$) and of second order ($3VK_2$), $T = 2$.

The solution $(\hat\rho_{1,0}, \hat\rho_{2,0}, \hat\rho_{3,0}, \hat\rho_{4,0})$ of the Riemann's problem at the junction for data $(\rho_1, \rho_{1,0}, \rho_{2,0}, \rho_{3,0}, \rho_{4,0})$ reads (see for instance Figures 14 and 18):

$$
\begin{aligned}
&f(\hat\rho_1) = f(\rho_1), \quad f(\hat\rho_2) = \tfrac{f(\sigma)-(1-\alpha_1)f(\rho_1)}{1-\alpha_2},\\
&f(\hat\rho_3) = \tfrac{\alpha_1-\alpha_2}{1-\alpha_2} f(\rho_1) + \tfrac{\alpha_2}{1-\alpha_2} f(\sigma), \quad f(\hat\rho_4) = f(\sigma),
\end{aligned}
\tag{3.13}
$$

with $0 \le \hat\rho_3 \le \sigma \le \hat\rho_2 \le 1$.
Hence, if $\rho_1 \to \rho_{1,0} = \sigma$ then

$$f(\hat\rho_3) \to \frac{\alpha_2}{1-\alpha_2} f(\sigma) = f(\rho_{3,0})$$

and $\hat\rho_3 \to \tau(\rho_{3,0})$. Therefore we can produce a wave on road 3 with strength bounded away from zero using an arbritrarily small wave on road 1.

Remark 3.2 The perturbation introduced on road 1, in order to have the solution described in (3.13), must lie in the interval

$$\tilde\rho_1 \le \rho_1 < \sigma,$$

with $\tilde\rho_1$ determined as the value such that

$$(1-\alpha_1) f(\tilde\rho_1) + (1-\alpha_2) f(\sigma) = f(\sigma),$$

that is to say

$$f(\tilde\rho_1) = \frac{\alpha_2}{1-\alpha_1} f(\sigma) = f(\sigma).$$

In the particular case we considered, we have

$$\tilde\rho_1 = \frac{\sqrt{2}-1}{2\sqrt{2}} \sim 0,146\ .$$

■

Notice that reducing the width of the perturbation on road 1, the total variation, principally represented by $\rho_{30} - \tau(\rho_{30})$ does not decrease, while the total variation on road 2 is tending to zero as $\rho_1 \to \rho_{1,0} = \sigma$.

3.3. **Junction with 2 incoming and 1 outgoing roads.** Recall rule (C) of the modeling at the junctions. Consider a crossing with two incoming roads and one outgoing road all parametrized by $[0, 1]$ and fix a right of way parameter $q \in]0, 1[$.

$$\begin{aligned} &\rho_{1,0} = 0.25, \quad \rho_{2,0} = 0.4, \quad \rho_{3,0} = 0.5, \\ &\rho_{1,b}(0,t) = 0.25, \quad \rho_{2,b}(0,t) = 0.4 \ . \end{aligned} \tag{3.14}$$

In the following Figures we represent road 3 in the upper graph, road 1 on the lower left graph and road 2 on the lower right one. The numerical solutions have been generated by the Godunov's method.
The initial data is depicted in Figure 19.
First we take $q = 0.5$ (see Figure 20). Both the incoming roads have the same right of way parameter: the density increases on road 1 and road 2 and becomes considerably high, while the density on road 3 remains constant.
Then assume $q = 0.25$ and observe the situation described in Figure 21. In the case represented in Figure 21 road 2 has the right of way parameter equal to $1 - q = 0.75$. It is easy to see that the density becomes very high on road 1, since road 2 has the priority to pass; the density is high on road 2 and remains the same on road 3.
Now take $q = 0.75$. Figure 22 shows that road 1 preserves its value of density, together with road 3, while road 2 reaches a very high value of density, due to the fact that its right of way parameter is $1 - q = 0.25$.

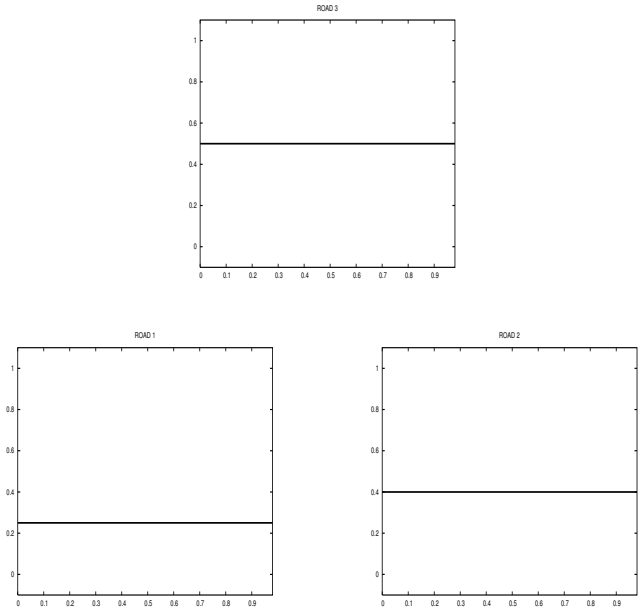

FIGURE 19. 1 outgoing and 2 incoming roads with $q = 0.5$, $h = 0.0125, T = 0$.

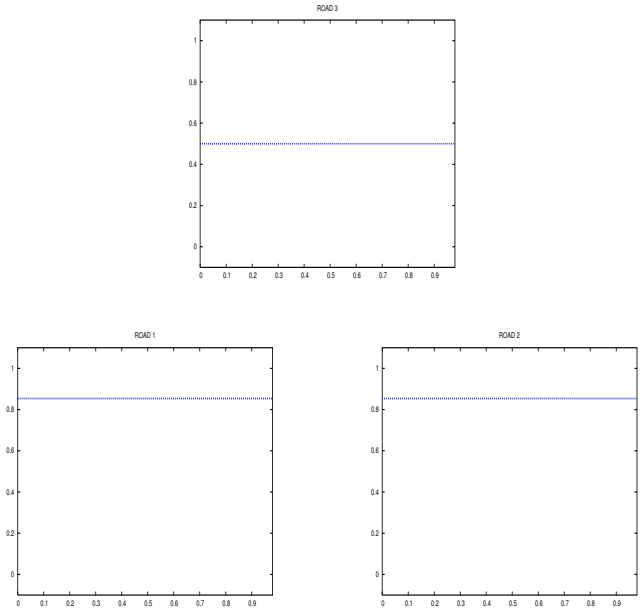

FIGURE 20. 1 outgoing and 2 incoming roads with $q = 0.5$, $h = 0.0125, T = 10$.

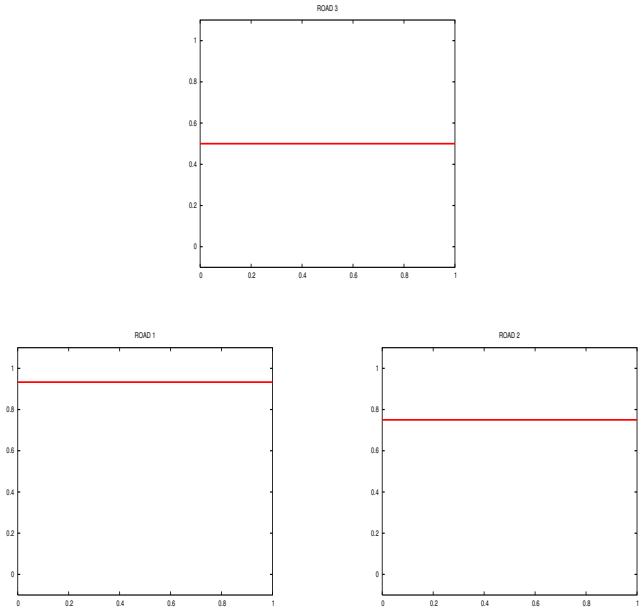

FIGURE 21. 1 outgoing and 2 incoming roads with $q = 0.25$, $h = 0.0125, T = 10$.

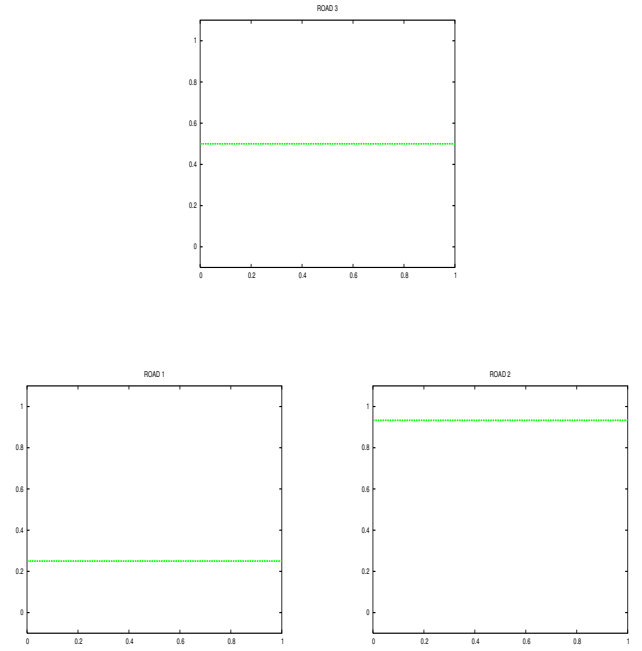

FIGURE 22. 1 outgoing and 2 incoming roads with $q = 0.75$, $h = 0.0125, T = 10$.

In the following table are reported orders and errors for data (3.14).

	G		$3VK_1$		$3VK_2$	
h	γ	L^1 Error	γ	L^1 Error	γ	L^1 Error
0.1	0.738593	0.009851	0.792745	0.009130	1.458312	0.009001
0.05	0.839375	0.005904	0.879531	0.005270	1.560714	0.003214
0.025	0.895055	0.003300	0.936022	0.002865	1.581739	0.000812
0.0125	0.929770	0.001774	0.968897	0.001497	1.524962	0.000473
0.00625	0.952295	0.000931	0.985818	0.000765	1.572714	0.000101
0.003125	0.983923	0.000481	0.9972134	0.000386	1.560145	0.000072

TABLE Convergence order γ, defined in (3.1), and errors of the approximation schemes Godunov (G), 3 velocities Kinetic methods of first order ($3VK_1$) and of second order ($3VK_2$) for data 3.14, $q = 0.25$, $T = 1$.

Bottleneck tests.
Now we want to present some numerical approximations to the equation (2.25) with fluxes

$$f_1(\rho) = \rho(1-\rho), \quad \rho \in [0,1], \tag{3.15}$$

on the widest part of the road and

$$f_2(\rho) = \rho\left(1 - \frac{3}{2}\rho\right), \quad \rho \in [0, 2/3] \tag{3.16}$$

on the narrowest part of the street.
The next tables provide a comparison between the three methods in temrs of L^1-error and order of convergence γ.
From now on, we assume to deal with a road of length 2 parametrized by the interval $[0,2]$ and that the separation point is placed in the middle of the road, namely at $x = 1$. The numerical schemes used to provide the approximated solution are Godunov's scheme (G), three-velocities Kinetic scheme of first order ($3VK_1$) and three-velocities Kinetic scheme of second order with the following velocities: $\lambda_3 = -\lambda_1 = 1.0$ and $\lambda_2 = 0$ ($3VK_2$).

Test B1. Let us assume the road is initially empty and take the following initial and boundary data

$$\rho_1(x,0) = \rho_2(x,0) = 0,$$
$$\rho_{1,b}(0,t) = 0.22\ .$$

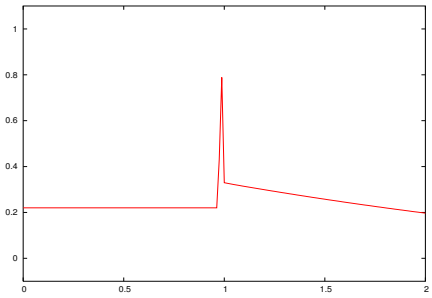

FIGURE 23. High level of car density at the interface, $h = 0.0125$, $T = 4$.

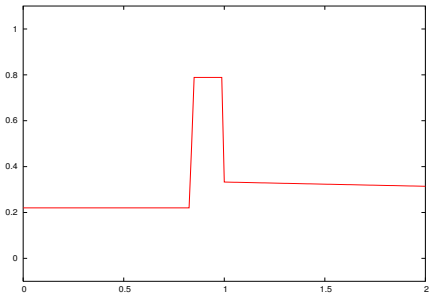

FIGURE 24. Shock propagating backwards, $h = 0.0125$, $T = 20$.

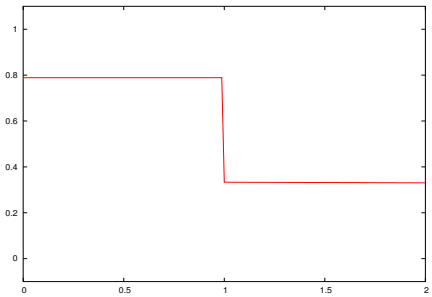

FIGURE 25. Shock reaches the boundary: heavy traffic, $h = 0.0125$, $T = 120$.

Since $\rho_{1,b} > \bar{\rho} \simeq 0.21$, in this case there is a jam formation as showed by the Figures 23, 24, 25.
A comparison between the three schemes is represented in Figure 26.

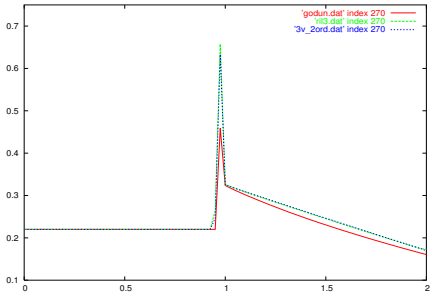

FIGURE 26. Comparison between the three numerical schemes $G, 3VK_1, 3VK_2$ for test B1, $h = 0.025$, $T = 3.375$.

In the next table we put orders and L^1-errors in the approximation of test B1.

	G	$3VK_1$	$3VK_2$
h	L^1 Error	L^1 Error	L^1 Error
0.1	0.012536	0.001211	0.001138
0.05	0.008575	0.007218	0.005219
0.025	0.005575	0.004720	0.002150
0.0125	0.003418	0.003166	0.000911
0.00625	0.002374	0.002242	0.000623
0.003125	0.001824	0.001635	0.000354

TABLE B1: Convergence order γ, defined in (3.1), and errors of the approximation schemes Godunov (G), Kinetic of first order ($3VK_1$) and of second order ($3VK_2$) for test B1 for $T = 2$.

Test B2. Assume again that the road is initially empty and take the following initial and boundary data

$$\rho_1(x,0) = \rho_2(x,0) = 0,$$
$$\rho_{1,b}(0,t) = 0.2\ .$$

Since $\rho_{1,b} < \bar{\rho}$, car density level is bounded, thus describing a situation of low traffic. See the next Figures 27, 28, 29.

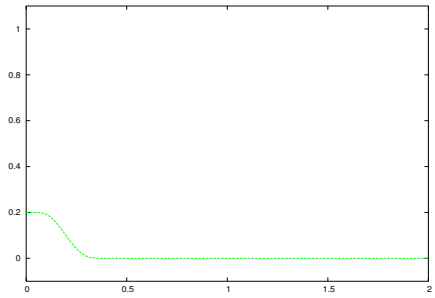

FIGURE 27. Traffic is entering on the left, $h = 0.0125$, $T = 0.25$.

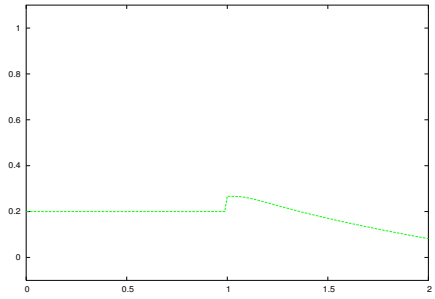

FIGURE 28. Density increases at the interface, $h = 0.0125$, $T = 1$.

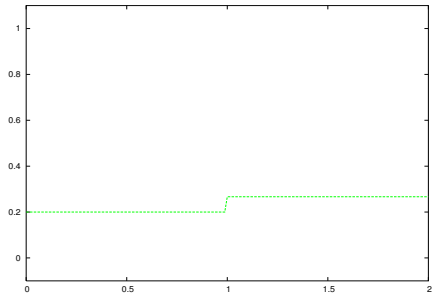

FIGURE 29. Low and stable traffic, $h = 0.0125$, $T = 10$.

Errors of the three methods are compared in the table below.

	G	$3VK_1$	$3VK_2$
h	L^1 Error	L^1 Error	L^1 Error
0.1	0.011227	0.010016	0.008050
0.05	0.009650	0.008736	0.005081
0.025	0.005111	0.004852	0.002179
0.0125	0.003310	0.00212	0.000822
0.00625	0.002080	0.001080	0.000583
0.003125	0.001270	0.001013	0.000201

TABLE B2: Orders and errors of the approximation schemes Godunov (G), Kinetic of first ($3VK_1$) and second order ($3VK_2$) for test B2, $T = 2$.

Test B3. Let us take the following initial and boundary data

$$\rho_1(x,0) = 0.66, \qquad \rho_2(x,0) = 0.66, \tag{3.17}$$
$$\rho_{1,b}(0,t) = 0.25\ .$$

The initial value 0.66 it is very close to the maximum value that can be absorbed by road 2, therefore, after a short time, namely $T = 2$, it can be observed the formation of a traffic jam.

The table of orders and errors follows.

	G		$3VK_1$		$3VK_2$	
h	γ	L^1 Error	γ	L^1 Error	γ	L^1 Error
0.1	0.573596	0.026991	0.766638	0.027383	1.092822	0.035529
0.05	1.047749	0.018136	1.428234	0.016096	1.433881	0.016657
0.025	0.529083	0.012031	0.632460	0.005981	0.976373	0.006165
0.0125	1.143648	0.004299	1.344904	0.003858	1.387269	0.002135
0.00625	0.613647	0.002580	0.674023	0.001559	0.939099	0.000858
0.003125	1.106762	0.001033	1.213628	0.000952	1.227004	0.000415

TABLE B3: Orders and errors of the approximation schemes Godunov (G), Kinetic of first order ($3VK_1$) and of second order ($3VK_2$) for test B3, $T = 1.5$.

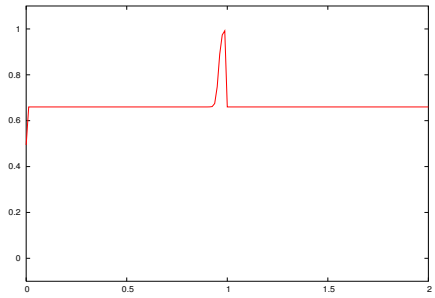

FIGURE 30. High level of car density at the interface, $h = 0.0125$, $T = 0.1$.

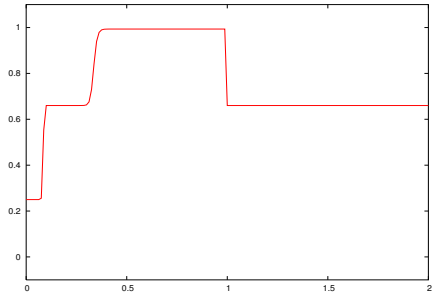

FIGURE 31. Shock propagating backwards, $h = 0.0125$, $T = 1$.

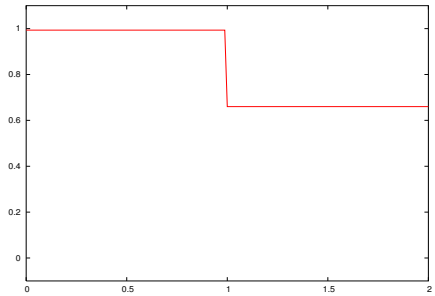

FIGURE 32. Shock reaches the boundary, traffic gets stuck, $h = 0.0125$, $T = 2$.

Next Figures compare the Godunov's method respectively with the Kinetic scheme of first order $(3VK_1)$ and the kinetic of second order $(3VK_2)$.

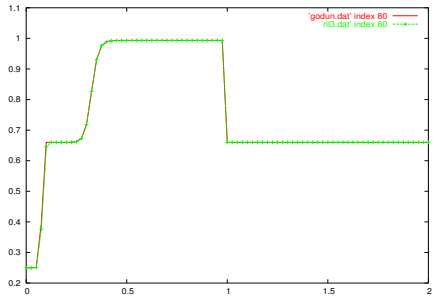

FIGURE 33. (G) scheme with line and $(3VK_1)$ with linepoints, $h = 0.025$, $T = 1$.

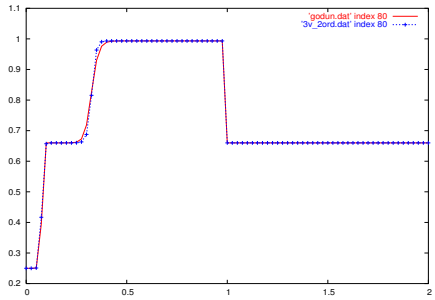

FIGURE 34. (G) scheme with line and $(3VK_2)$ with linepoints, $h = 0.025$, $T = 1$.

3.4. **Traffic circles.** In the next pages we present some simulations reproducing a simple traffic circles composed by 8 roads and 4 junctions. The numerical solutions have been generated by the Godunov's method for $h = 0.025$ and $cfl = 0.5$.

TC1: heavy traffic. Consider first the following initial and boundary data

$$\begin{aligned} \rho_1(x,0) &= 0.25,\ \rho_2(x,0) = 0.4,\ \rho_3(x,0) = 0.5,\ \rho_4(x,0) = 0.5, \\ \rho_{1R}(x,0) &= 0.5,\ \rho_{2R}(x,0) = 0.5,\ \rho_{3R}(x,0) = 0.5,\ \rho_{4R}(x,0) = 0.5, \\ \rho_{1,b}(0,t) &= 0.25, \quad \rho_{2,b}(0,t) = 0.4\ . \end{aligned}$$

Let us set the right of way parameters $q_1 = q(1, 4R, 1R) = 0.75$, $q_2 = q(2, 2R, 3R) = 0.75$. This means that road 1 is the through street respect to road $4R$ and road 2 is the through street respect to $2R$. The distribution coefficients $(\alpha_{1R,3}, \alpha_{1R,2R}, \alpha_{3R,4}, \alpha_{3R,4R})$ are assumed to be constant and are all equal to $\alpha = 0.5$. Let us see the evolution of traffic in time in Figures 35, 36, 37, 38. In particular, one can observe that at time $t = 10$ the chosen right of way parameters provoke shocks propagating backwards along roads $2R$ and $4R$ and consequently a shock is created on road 2. Successively, the density on roads $4R$, $2R$ increases and shocks are propagating backwards on roads $1R$ and $3R$. Roads 3 and 4 show a very low density of cars. At $T = 40$ we see that the traffic jam is formed in the traffic circle, thus the outgoing roads 3 and 4 are empty.

Then, consider the same initial and boundary data above. As before, the distribution coefficients $(\alpha_{1R,3}, \alpha_{1R,2R}, \alpha_{3R,4}, \alpha_{3R,4R})$ are assumed to be constant and are all equal to $\alpha = 0.5$. Here the right of way parameters are $q_1 = q(1, 4R, 1R) = 0.25$, $q_2 = q(2, 2R, 3R) = 0.25$. This means that road $4R$ is the through street respect to road 1 and road $2R$ is the through street respect to 1. The evolution of traffic in time is reported in the next Figures 35, 39, 40, 41.
Observe that at time $t = 5$ shocks are generated on the entering roads 1 and 2, while rarefaction waves in the direction of traffic are created on roads $4R$, $2R$, 3, 4. Roads $1R$ and $3R$ mantain the same level of density. At $t = 10$ the rarefaction waves traveling in the sense of traffic produce a decrease in the car density on roads $4R$, $3R$, 3, 4. On entering roads 1 and 2, the effect of the shocks traveling backwards is a considerable increase of the density and again, roads $1R$ and $3R$ mantain the same level of density. At time $T = 40$ the roads entering in the circle are blocked, while on the outgoing roads 3 and 4 the density is low.
Notice that in both the considered examples the choice of the right of way parameter cause a traffic jam on the roads entering the junction.

Density at time t = 0.1

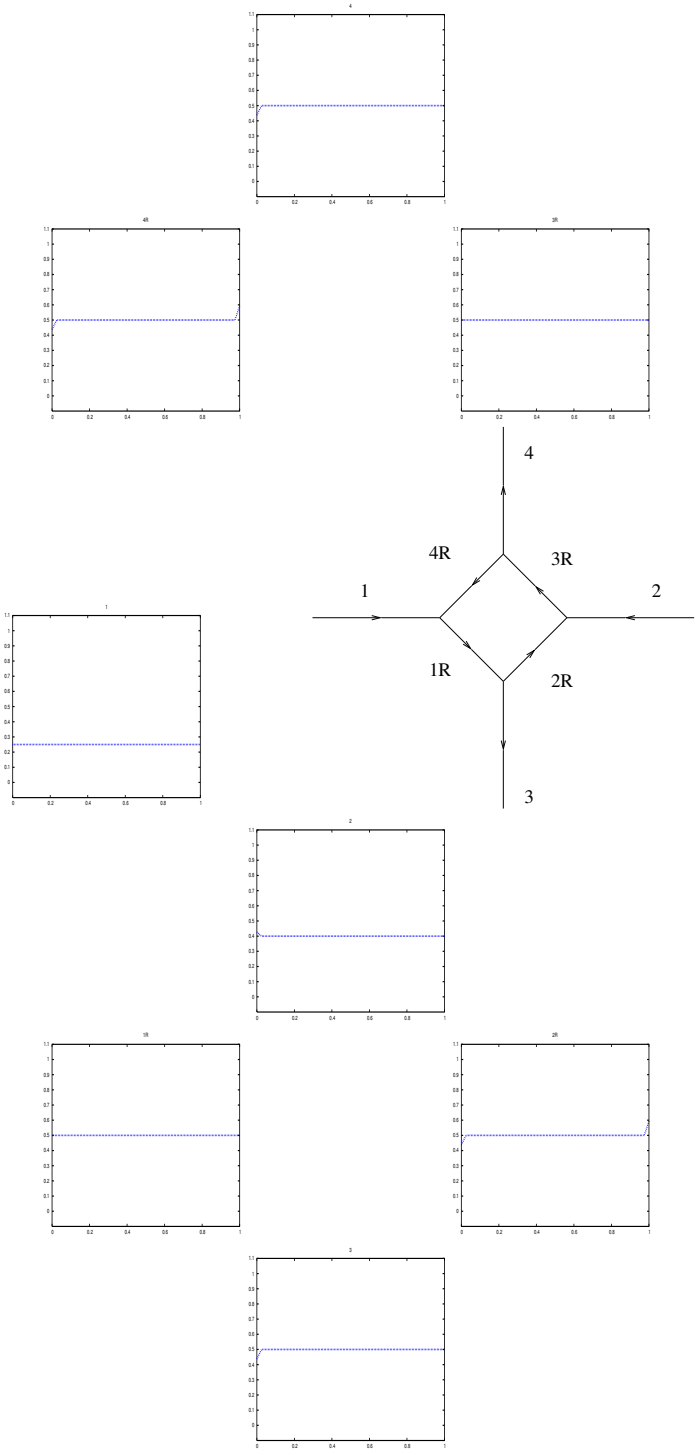

FIGURE 35. Traffic circle at $t = 0.1$.

Density at time t = 10

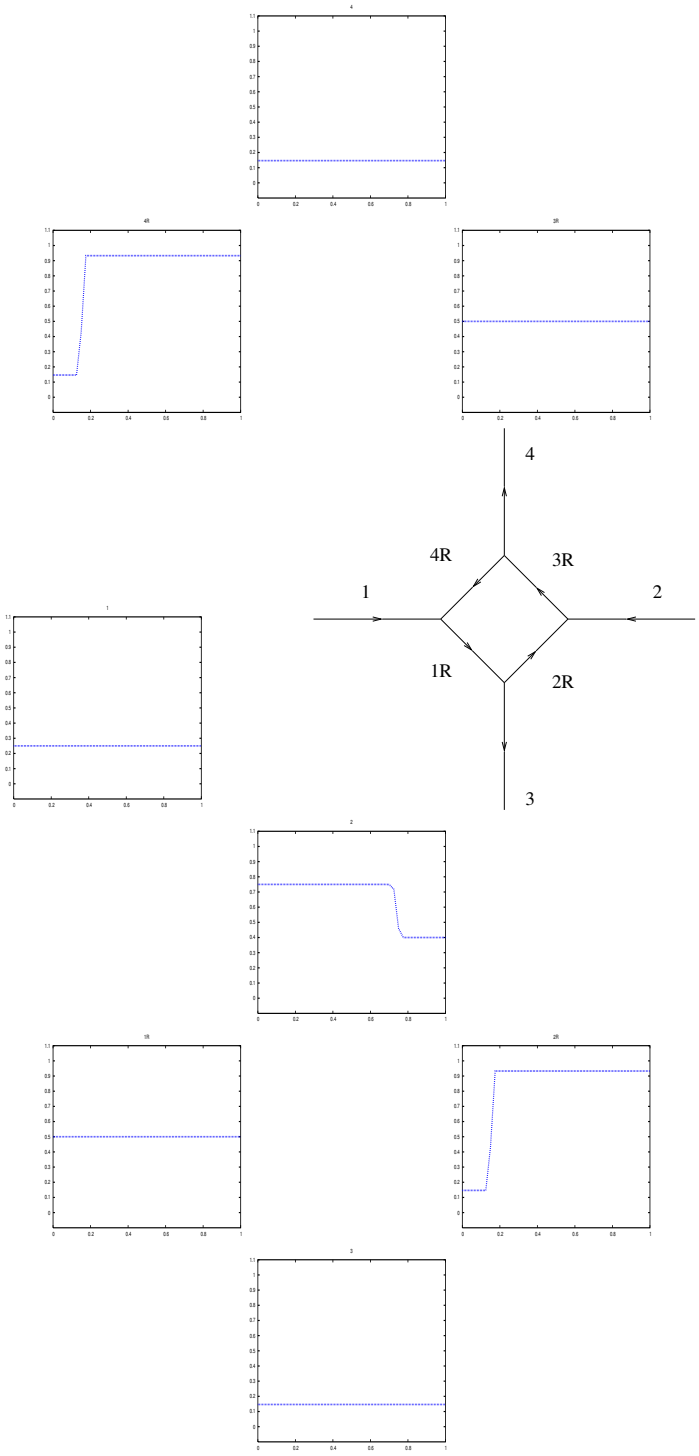

FIGURE 36. Traffic circle at $t = 10$: due to the values of the right of way parameters q_1 and q_2, shocks are propagating backwards along roads $2R$ and $4R$, and consequently a shock is created on road 2 .

Density at time t = 20

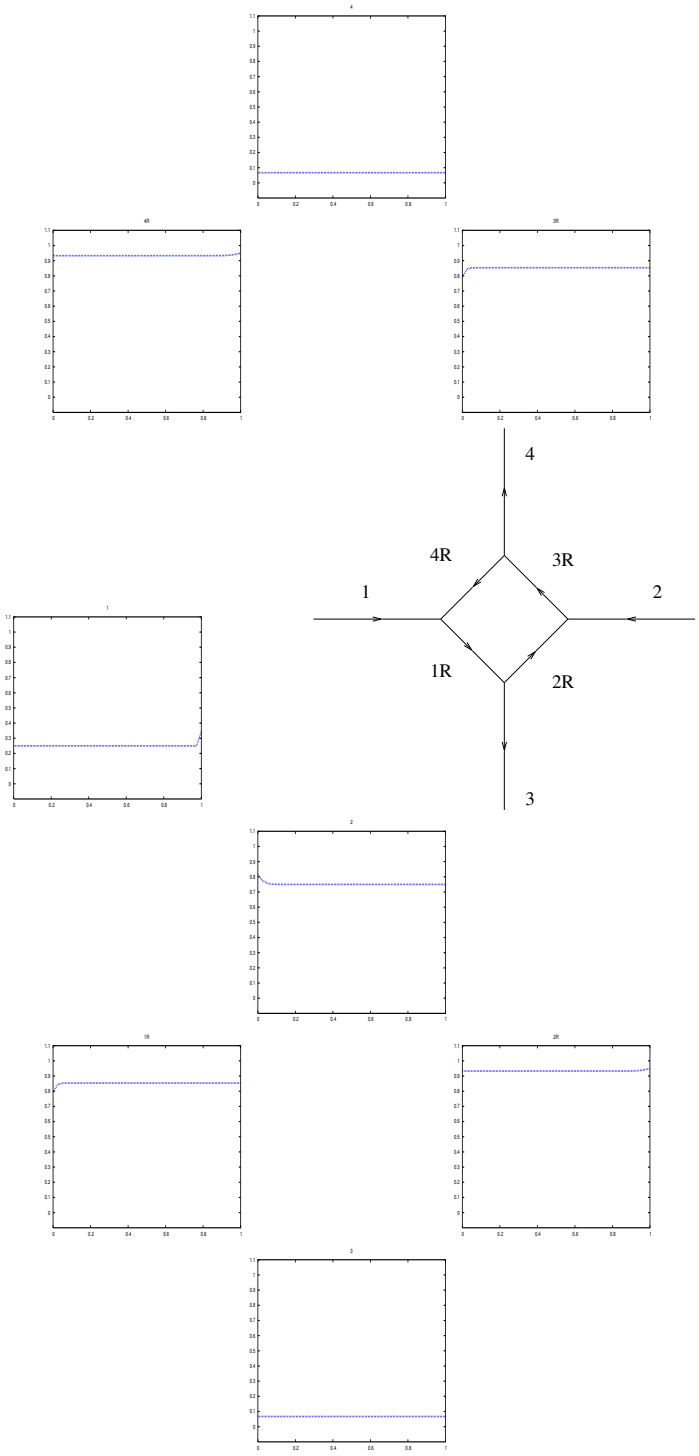

FIGURE 37. Traffic circle at $t = 20$: density is high on roads $4R$, $2R$. Shocks are propagating backwards on roads $1R$ and $3R$ and on the incoming roads 1 and 2. On the outgoing roads 3 and 4 the density is low .

Density at time t = 40

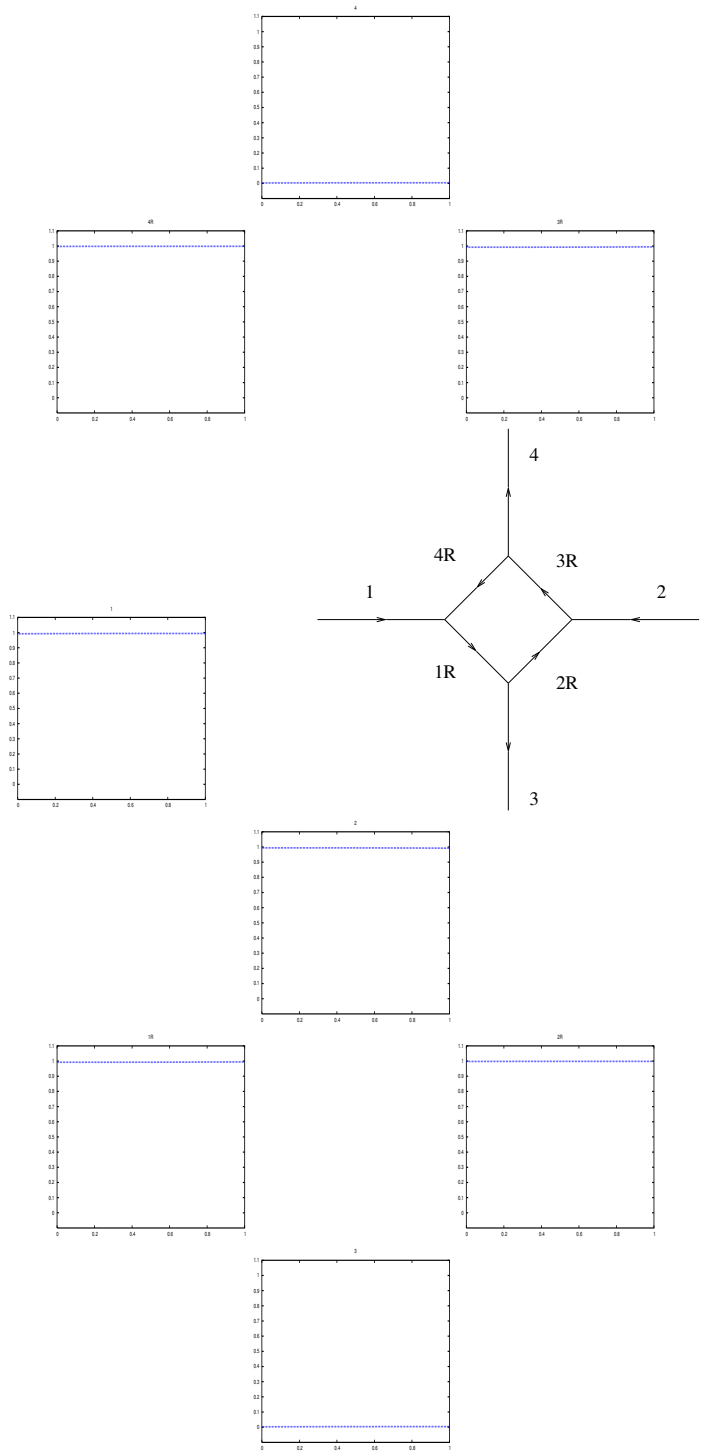

FIGURE 38. Traffic circle at $T = 40$: traffic is blocked on the entering roads, namely road 1 and 2 and on the roads of the circle, the outgoing roads become empty.

Density at time t = 5

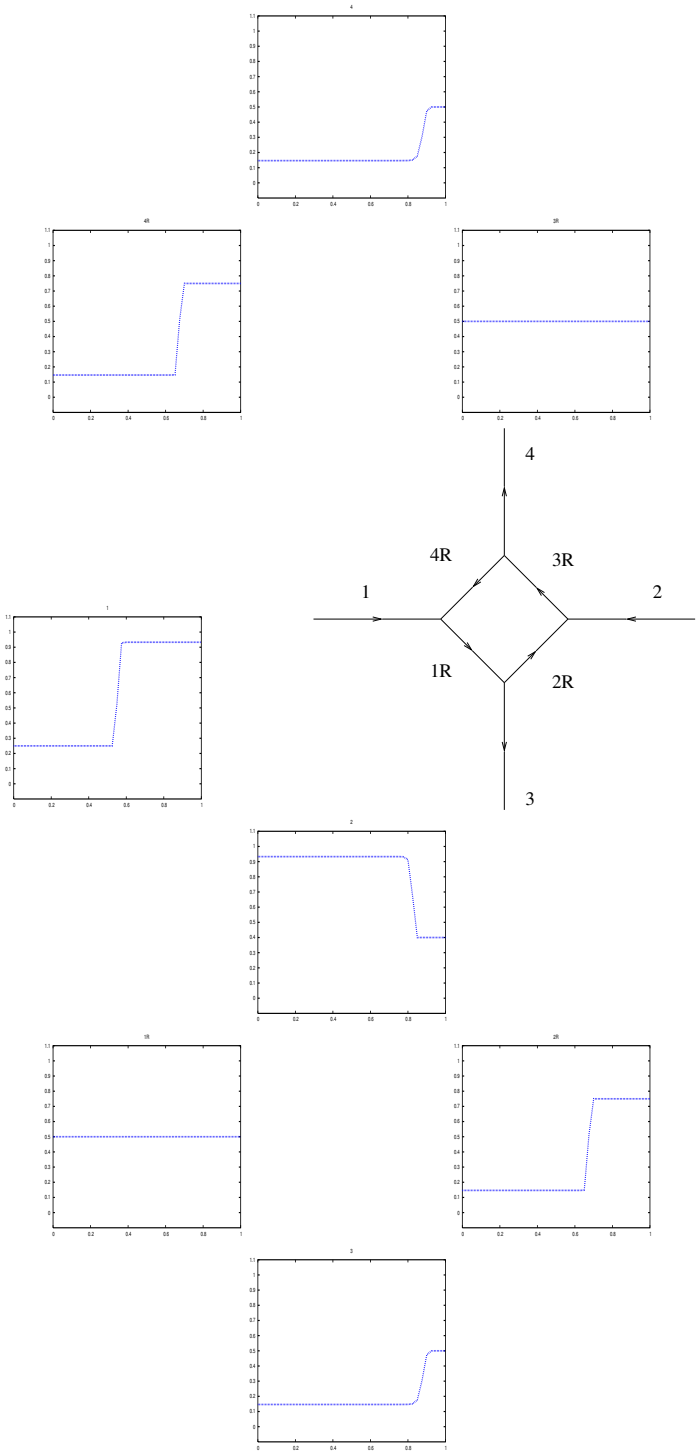

FIGURE 39. Traffic circle at $t = 5$: shocks are generated on the entering roads, while rarefaction waves in the direction of traffic are created on roads $4R$, $2R$, 3, 4 .

Density at time t = 10

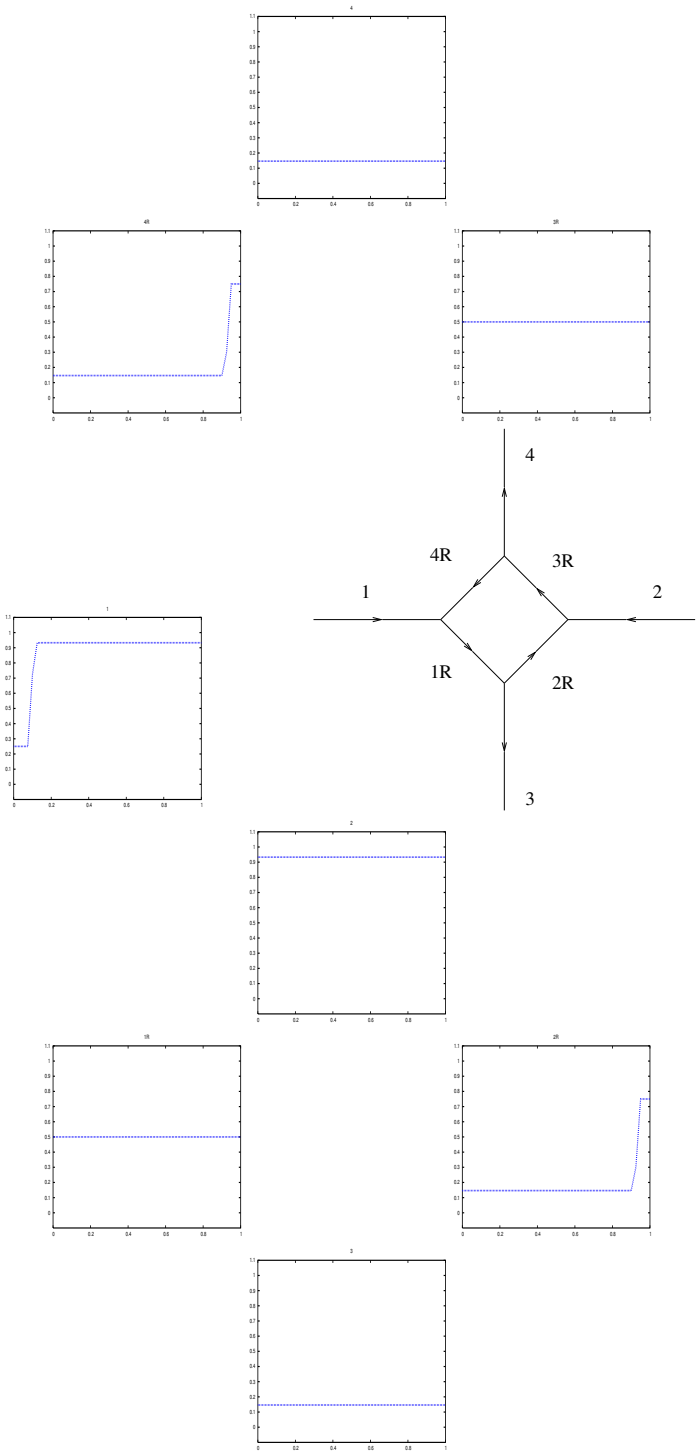

FIGURE 40. Traffic circle at $t = 10$: density of cars is lowered on roads $4R$, $3R$, 3, 4 and it is very high on the roads entering the circle.

Density at time t = 40

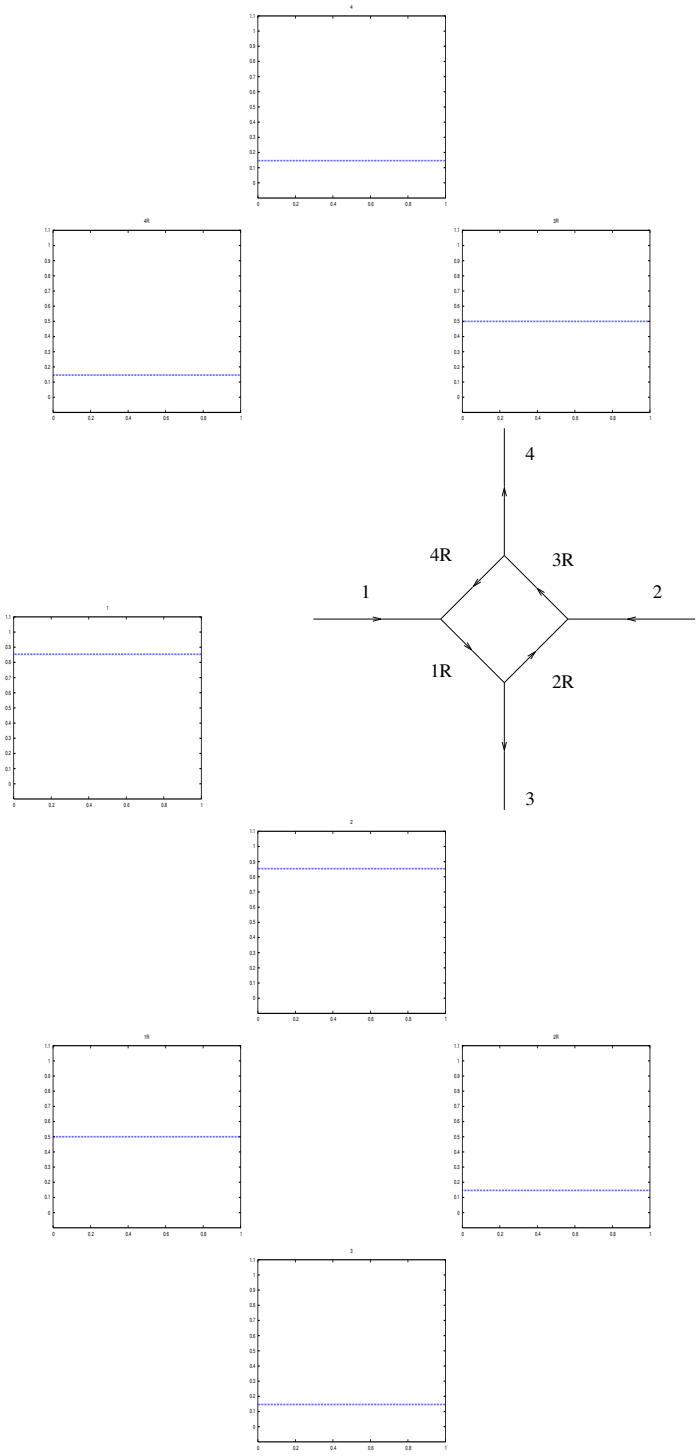

FIGURE 41. Traffic circle at $T = 40$: the roads entering in the circle, namely road 1 and 2, are blocked, while on the outgoing roads 3 and 4 and also on $4R, 2R$ the density is low. On the roads $1R, 3R$ the density is normal.

Let us now take a portion of urban network. In particular, we consider a crucial area for traffic in the city of Rome, which is represented by the Square of "Re di Roma", showed in Fig. 42.

FIGURE 42. Re di Roma.

Note that in this case we deal with a network composed by 24 roads and 12 junctions. The next figures show the simulations performed by the Godunov's scheme with space step $h = 0.01$, cfl 0.5, final time $T = 20$. The network is initially empty and on each incoming road we put a low boundary density equal to $\rho_b = 0.1$. The right of way parameters, necessary for the junctions with only one outgoing road are fixed to $q = 0.5$, while the distribution coefficients are chosen taking into account the different importance between the roads composing the circle. The values of the density can be individuated through the different colours along the roads(light colours correspond to low density, dark colours to high density).
Since at the beginning the network is initially empty, we see that the density in the traffic circle for $t = 0.25$ is zero, as underlined by the white color. After a certain time, the traffic on the roads within the circle is congested and the traffic jam starts propagating backwards.

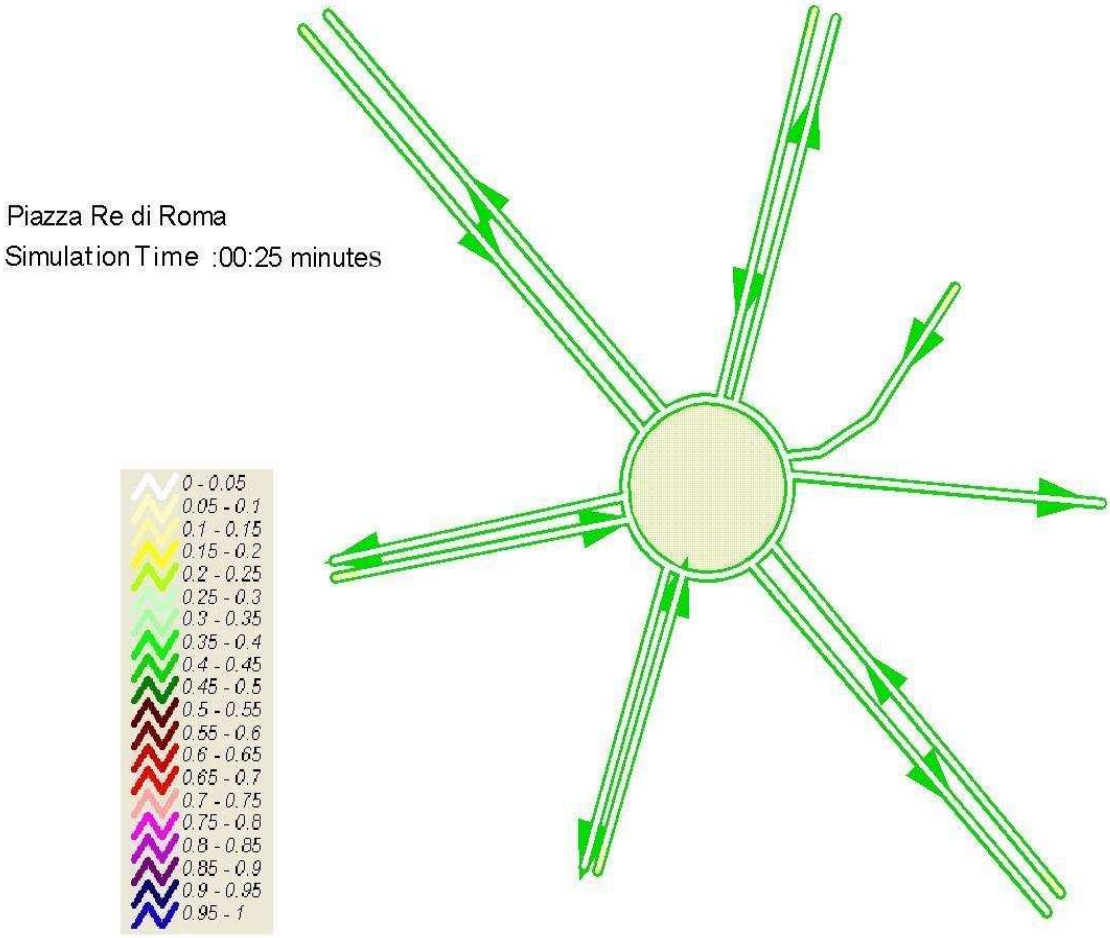

FIGURE 43. Re di Roma simulation, t=0.25.

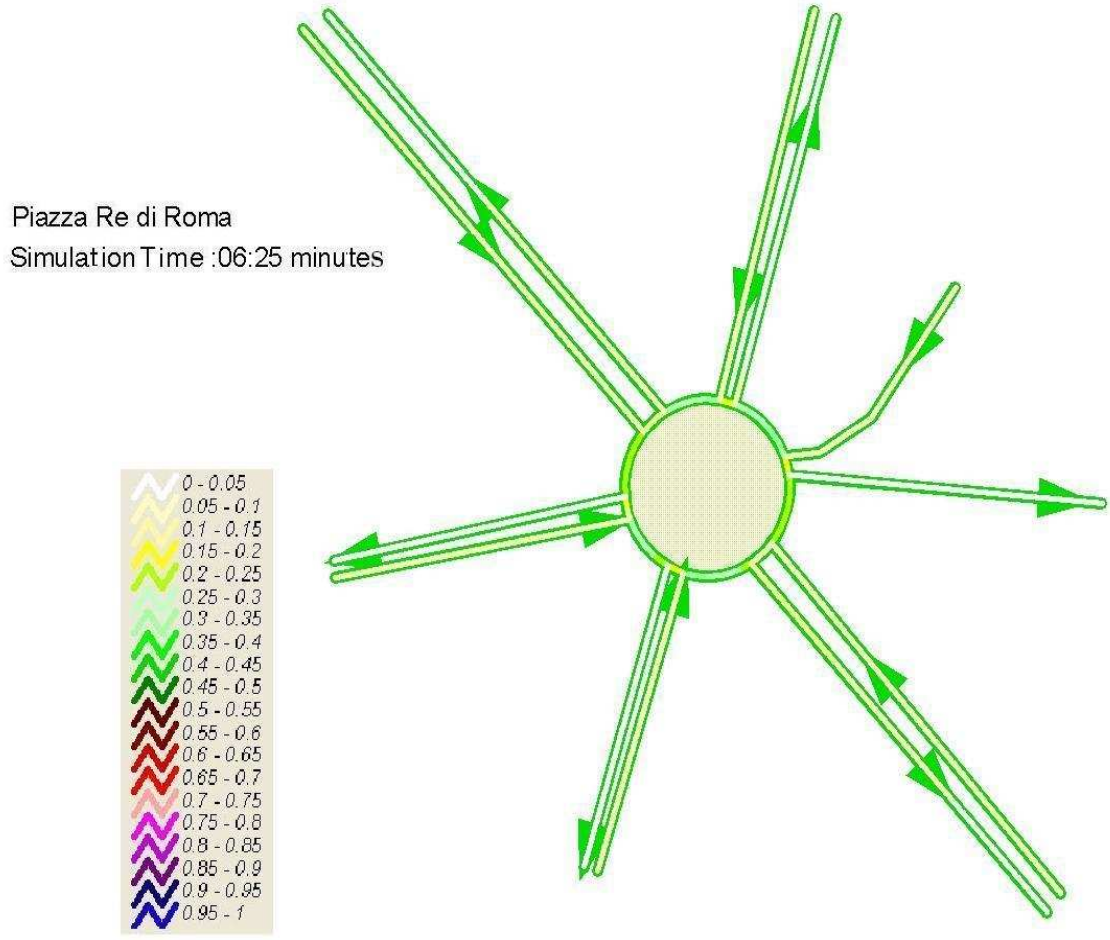

FIGURE 44. Re di Roma simulation, t=6.25.

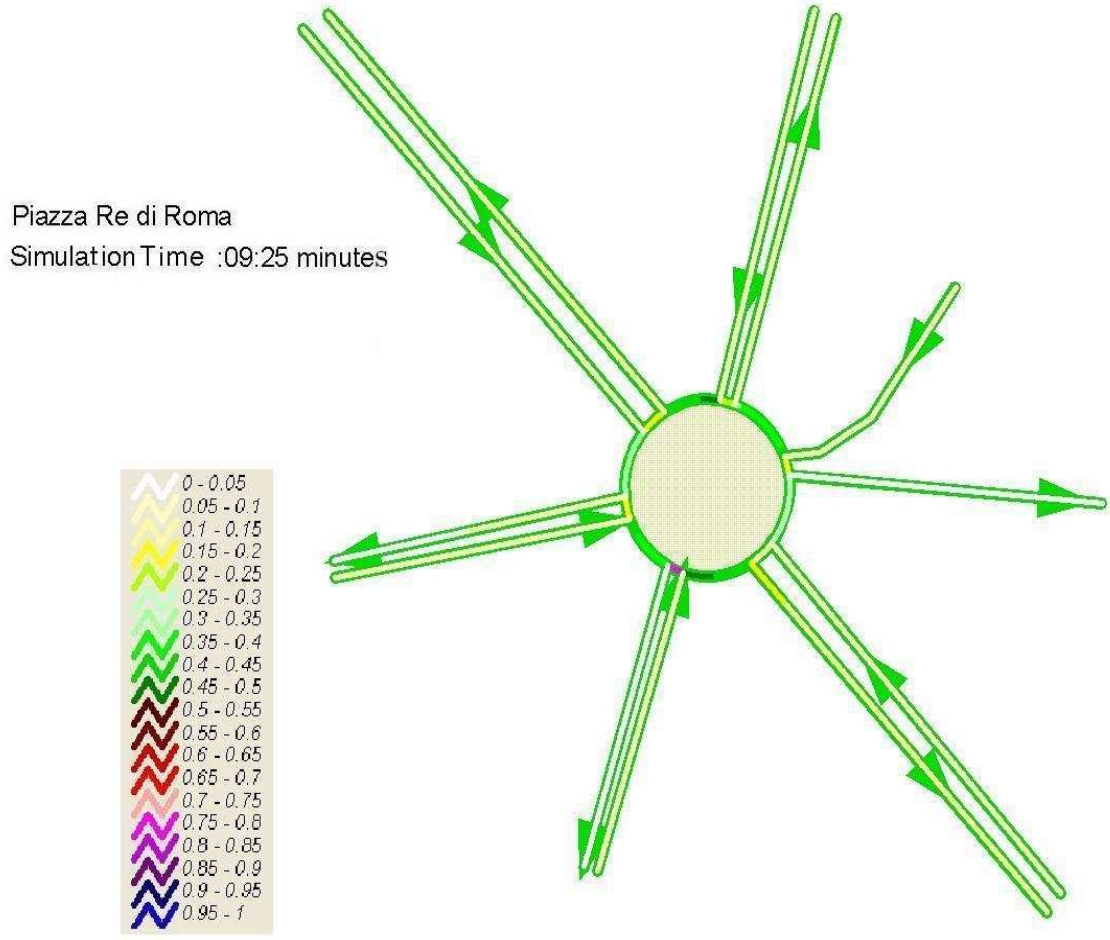

FIGURE 45. Re di Roma simulation, t=9.25.

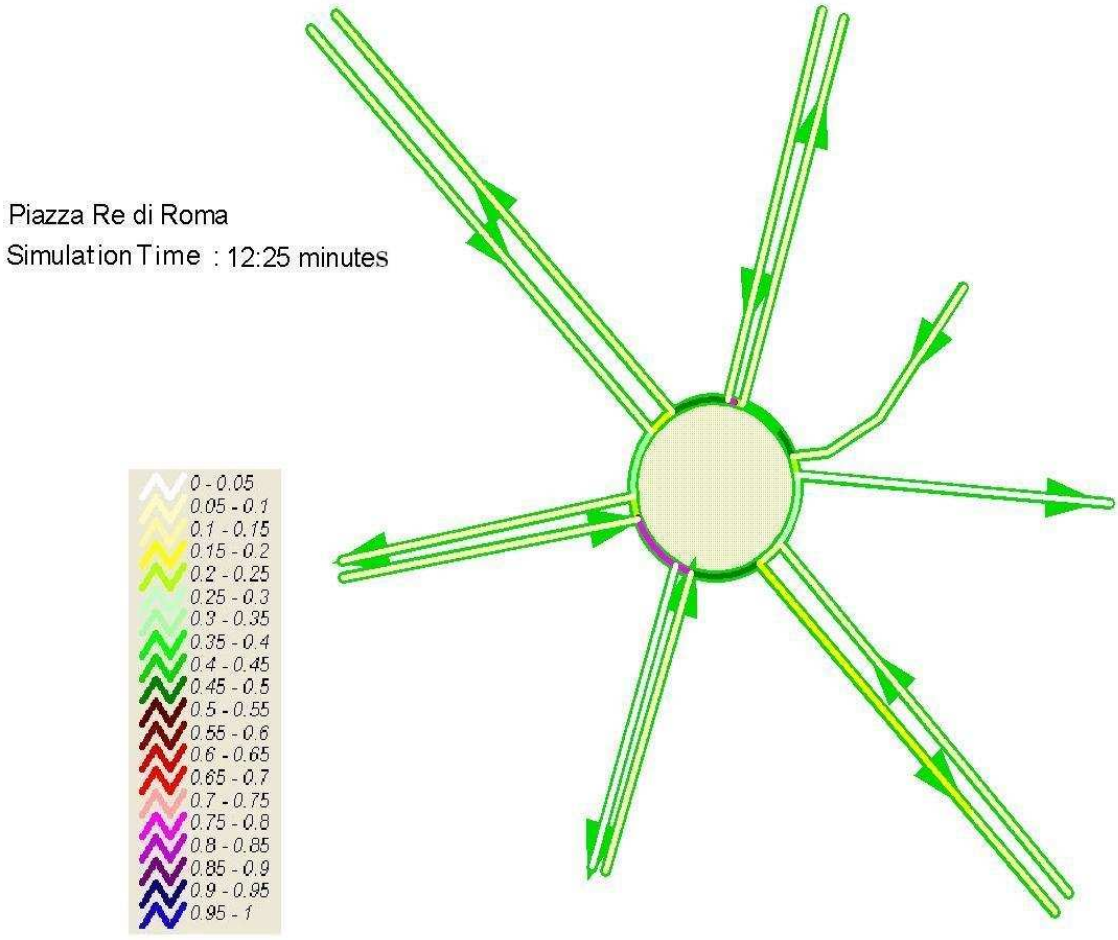

FIGURE 46. Re di Roma simulation, t=12.25.

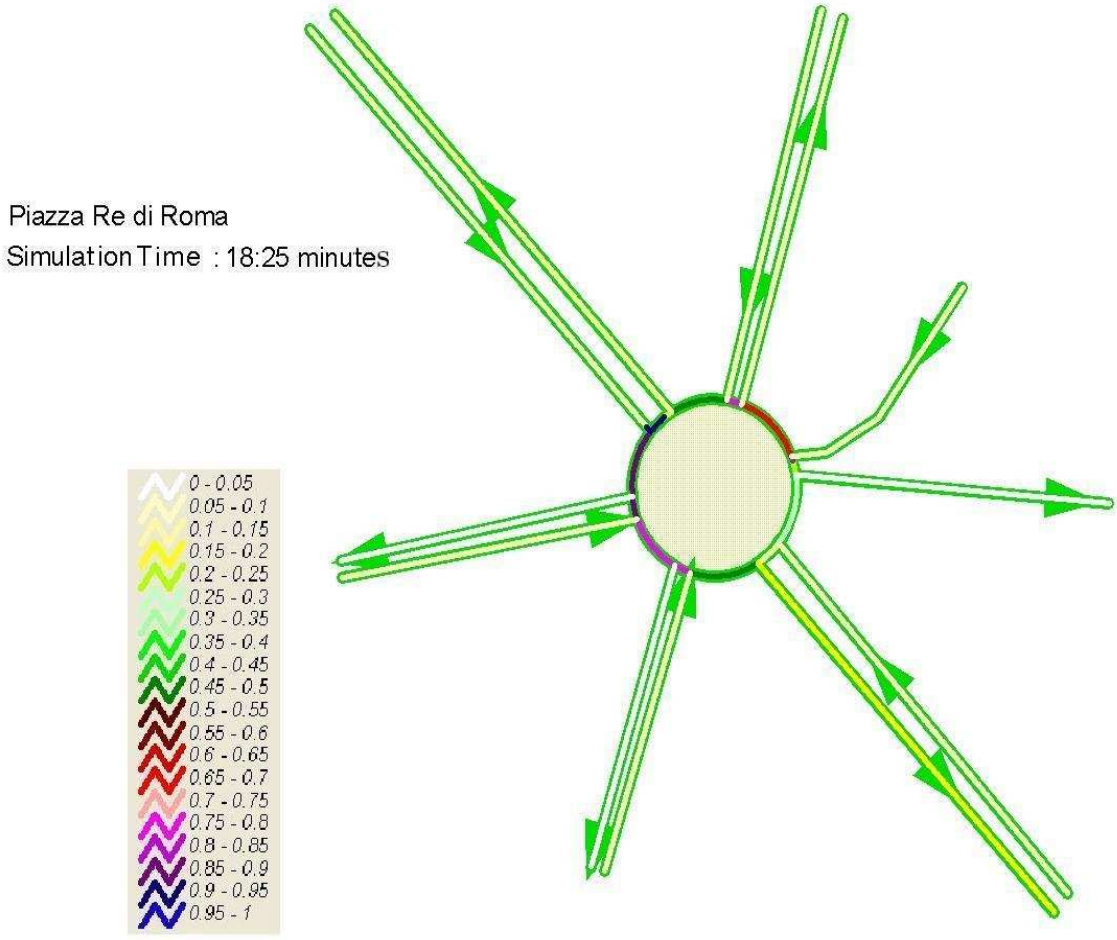

FIGURE 47. Re di Roma simulation, t=18.25.

References

[1] D. Aregba-Driollet, V. Milišić. Kinetic Approximation of a Boundary Value Problem for Conservation Laws. *Numerische Mathematik* **97** (2004), 595-633.

[2] D. Aregba-Driollet, R. Natalini. Discrete Kinetic Schemes for Multidimensional Systems of Conservation Laws. *SIAM J. Numer. Anal.* **37** (2000), No. 6, 1973-2004.

[3] C. Bardos, A. Y. Le Roux and J. C. Nédélec. First order quasilinear equations with boundary conditions. *Comm. Partial Differential Equations* **4** (1979), 1017-1034.

[4] G. M. Coclite, M. Garavello, B. Piccoli. Traffic Flow on a Road Network. *Siam Math. Anal.* (to appear).

[5] Y. Chitour, B. Piccoli. Traffic circles and timing of traffic lights for cars flow. *Discrete and Continuous Dynamical Systems-Series B* (to appear).

[6] E. Godlewski, P. A. Raviart. Hyperbolic systems of conservation laws. Mathématiques & Applications [Mathematics and Applications], 3/4. Ellipses, Paris (1991).

[7] M. J. Lighthill, G. B. Whitham. On kinematic waves. II. A theory of traffic flow on long crowded roads. *Proc. Roy. Soc. London. Ser. A.*, **229** (1955), 317–345.

[8] R. Haberman. Mathematical models. Prentice-Hall, Inc. New Jersey, 1977, 255-394.

[9] R. Natalini. Convergence to Equilibrium for the Relaxation Approximations of Conservation Laws. *Comm. Pure Appl. Math.* **49** (1996), 795-823.

[10] R. Natalini. A Discrete Kinetic Approximation of Entropy Solutions to Multidimensional Scalar Conservation Laws. *Journal of differential equations*, **148** (1998), 292-317.

[11] R. Natalini. Recent results on hyperbolic relaxation problems, in Analysis of systems of conservation laws. ed. H. Freistűler, *Monographs and surveys in Pure and Applied Mathematics* **99**, Chapman-Hall/CRC (1999).

[12] P. I. Richards. Shock Waves on the Highway. *Oper. Res.*, **4** (1956), 42-51.